 doi:10.20944/preprints202008.0468.v1

Review

Quantification of atmospheric ammonia concentrations: A review of its measurement and modeling

Arshad Arjunan Nair and Fangqun Yu

Atmospheric Sciences Research Center, State University of New York at Albany
251 Fuller Road, Albany, NY 12203, USA
* Correspondence: aanair@albany.edu and fyu@albany.edu

Abstract: Ammonia (NH_3), the most prevalent alkaline gas in the atmosphere, plays a significant role in $PM_{2.5}$ formation, atmospheric chemistry, and new particle formation. This paper reviews quantification of [NH_3] through measurements, satellite-remote-sensing, and modeling reported in over 500 publications towards synthesizing current knowledge of [NH_3], focusing on spatiotemporal variations, controlling processes, and quantification issues. Most measurements are through regional passive sampler networks. [NH_3] hotspots are typically over agricultural regions like the Midwest US and North China Plain, with elevated concentrations reaching monthly averages of 20 and 74 ppbv, respectively. Topographical effects dramatically increase [NH_3] over the Indo-Gangetic Plains, North India and San Joaquin Valley, US. Measurements are sparse over oceans, where [NH_3] ≈ few tens of ppbv, variations of which can affect aerosol formation. Satellite-remote-sensing (AIRS, CrIS, IASI, TANSO-FTS, TES) provides global [NH_3] quantification in the column and at surface since 2002. Modeling is crucial for improving understanding of NH_3 chemistry and transport, its spatiotemporal variations, source apportionment, exploring physicochemical mechanisms, and predicting future scenarios. GEOS-Chem (global) and FRAME (UK) models are commonly applied for this. A synergistic approach of measurements↔satellite-inference↔modeling is needed towards improved understanding of atmospheric ammonia, of concern from the standpoint of human health and the ecosystem.

Keywords: review; ammonia; modeling; measurement; atmospheric chemistry; particle formation and $PM_{2.5}$

1. Introduction

Atmospheric ammonia (NH_3), mainly from agriculture with additional sources in industrial and vehicular emissions, plays a key role in many aspects of our environment by virtue of its alkalinity, reactivity, solubility, and abundance. In the recent years, there has been an increase in its concentration ([NH_3]) mainly due to increased land use for agriculture [1–3] to support our burgeoning population. This has generated concern about its negative impacts on the climate and human health. This is especially so due to the role of NH_3 in the formation of $PM_{2.5}$ through its neutralization of acidic species in the atmosphere. NH_3 has been receiving increasing attention recently due to its potential enhancement of atmospheric new particle formation [4,5]. The impacts of NH_3 as well as the resultant particulate matter on human health [6], the ecosystem, and climate deem understanding its concentration in the atmosphere important.

NH_3 has the following major impacts on the environment. Firstly, NH_3 is the greatest contributor to reactive nitrogen deposition [7–10] in several regions across the globe. Such deposition can contribute

Preprints (www.preprints.org) | NOT PEER-REVIEWED | Posted: 21 August 2020 doi:10.20944/preprints202008.0468.v1

to eutrophication of aquatic and terrestrial exosystems [11,12], which may be enhanced due to the greater bioavailability of NH_3 or ammonium (NH_4^+) compared to other reactive nitrogen species [13–15]. Acidification via nitrification, the conversion of NH_3 to nitrite (NO_2^-) and then to nitrate (NO_3^-), can also occur [11,12,16–21]. For instance, 1 mol of ammonium sulfate ($(NH_4)_2SO_4$) can potentially release 4 mols of acidity, i.e. H^+ ions. Secondly, NH_3 can have direct negative impacts on the ecosystem, which are expected above a critical threshold of ~4 ppbv of [NH_3] [22], which is frequently the case in several countries. They may directly affect vegetation [12,23] or livestock [24–26] or humans [27,28]. Thirdly, NH_3 plays a role in determining the total particle mass and number concentrations, apart from the extent of neutralization of atmospheric particles [4,29–31]. The contribution of NH_4^+ to particulate matter is comparable to that of other inorganic species such as NO_3^- and sulfate (SO_4^{2-}) as seen from modeling [32–34] and measurements [9,35,36]. Further, Tsigaridis *et al.* [33] indicate that the increase in NH_4^+ absolute (0.13 → 0.37 Tg) and relative (0.5% → 1.3%) contribution to aerosol burden from pre-industrial to present-day times, which is supported by observations from ice core studies [37–39]. NH_3 also affects hygroscopicity of particles, an important physicochemical property determining particles' water carrying capacity. Finally, NH_3 can significantly enhance the nucleation rate of aerosol particles through sulfuric acid vapor condensation [4,5,40–42], with implications to aerosol indirect radiative forcing. Further, gas-particle partitioning of NH_3 to form NH_4^+ salts can contribute to the continued growth of these newly-formed aerosol particles. Although NH_3 shows thermodynamic preference for neutralization of H_2SO_4 to form solid $(NH_4)_2SO_4$, formation of the semi-volatile NH_4NO_3 when there is small supersaturation of NH_3 and HNO_3 can contribute to rapid particle growth [43]. Additionally, NH_3 that remains in the gas-phase can dissolve into the aerosol water and increase its pH, thereby increasing the solubility of HNO_3 and other acidic species. Considering the largest uncertainties in climate modeling come from aerosols [44], the role of NH_3 in aerosol nucleation, growth, and characteristics are especially important. Further, the relatively shorter atmospheric lifetimes of its particulate forms implies that there may be more significant regional climate impacts [45].

Due to its importance, quantification of atmospheric [NH_3], mostly through in-situ measurements, satellite remote sensing, and modeling, has been reported in hundreds of publications. Here we review these previous studies, with the following aims: (1) aggregating current knowledge from the varied measurement techniques for the estimation of NH_3 in the atmosphere (2) identifying the variability and trends in [NH_3] (3) understanding these features in context of the processes that govern the concentration of ambient atmospheric NH_3 (4) examining the issues with these quantification approaches and the current and required attempts at resolving these. To the best of our knowledge, there has been no comprehensive review of previous studies of quantification of atmospheric NH_3 concentrations.

In the present section, we have provided the motivation for this review and a survey of literature examining atmospheric NH_3 and its effects. Figure 1 outlines this review: Section 2 details the various measurement techniques of atmospheric NH_3. Some key studies and their results are discussed here. Section 3 is on the modeling of NH_3 and the processes that affect its concentration in the atmosphere. This section also examines the validation of modeling studies with observations and some insights that this provides. Section 4 paints a picture of the spatial distribution on the global and regional scales. Section 5 examines the temporal trends in [NH_3] on varying scales from several studies that quantify NH_3. Issues with the various approaches of quantifying [NH_3] are discussed in each corresponding section and summarized in Section 6, which also concludes with the future steps and challenges in the quantification of atmospheric NH_3.

Preprints (www.preprints.org) | NOT PEER-REVIEWED | Posted: 21 August 2020 doi:10.20944/preprints202008.0468.v1

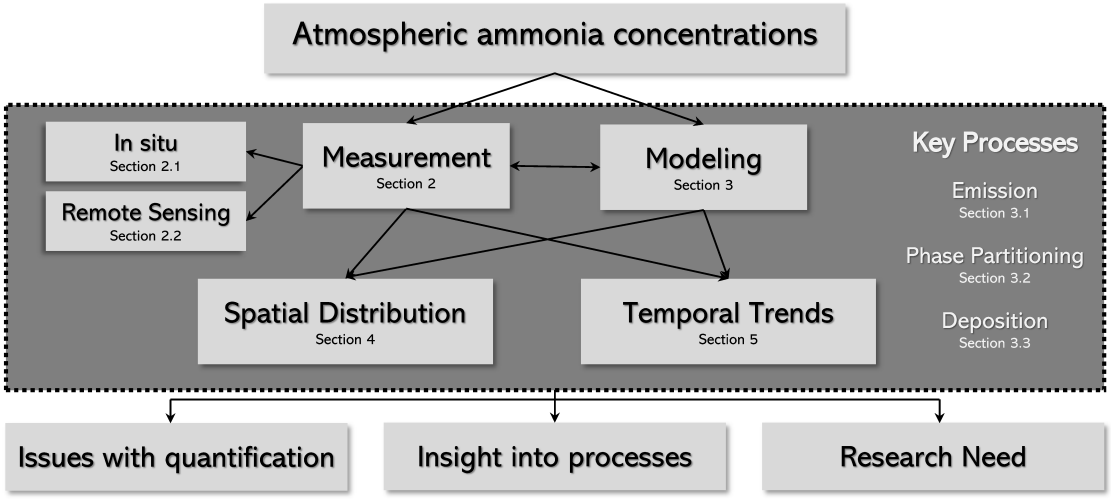

Figure 1. A schematic of the discussion in this review paper.

2. Measurement of [NH_3]

2.1. In situ measurements

It is natural that the first measurements of NH_3 in the gas-phase were made through ground-based instrumentation. The earliest detailed measurements of atmospheric NH_3 were made by Egner and Eriksson [46] over Scandinavia. "Ammonia and nitrate are determined in one aliquot of the sample by successive destillations in all-glass stills with excess of sodium hydroxide, and Devarda's alloy. The final estimate of ammonia is made with a special Nessler technique, using a photoelectric colorimeter." However, their approach did not distinguish the gas-phase NH_3 and the aerosol NH_4^+. The first measurements of [NH_3] solely in the gas-phase was by Junge [47] over locations in Florida and Hawaii, with an important realization that the NH_4^+ aerosol was formed from atmospheric NH_3. Over the next six decades, there have been advancements in measurement methods, initially aiming at distinguishing gas/aerosol phases and the later goal of realizing continuous measurement of [NH_3].

Towards the first goal, the first major development was the filter pack method [48], which filtered out aerosol particles on a Teflon pre-filter before collection of NH_3 on an acid-coated filter. However, there were issues with volatility of the aerosol NH_4^+ causing positive error, and humidity causing NH_3 deposition in the pre-filter and consequently a negative error in NH_3 measurement [49]. In 1979, Martin Ferm discussed a "method for determination of atmospheric ammonia" based on the differential diffusion rates to a surface for gas molecules and aerosols [50]. Using an oxalic acid-coated tube, separation of NH_3 (trapped onto the tube walls) and NH_4^+ aerosols is achieved. Many of the later refinements into NH_3 detection instruments have been based on this simple denuder technique. Continuous measurement of NH_3 was achieved by Wyers *et al.* [51], where a fully automated continuous flow rotating wet denuder was developed.

Numerous ground-based measurements of atmospheric NH_3 are listed in Table S1. The observations made in the reviewed literature are synthesized into Figure 2, with a global map of the average surface [NH_3] measurements ranging from < 1 ppbv in remote continental and oceanic areas to > 24 ppbv, typically over regions of intensive agriculture. Longer detailed measurements have been made over the United States, Europe, and China. Some of the important results and inferences from these studies are discussed in detail in subsequent sections. From Table S1 and Figure 2 we note that most in situ measurements of [NH_3] are over land. Most surface-based measurements over land are made in North America and Europe. Systematic measurements have been made through NH_3 monitoring networks, which have been established after identifying increasing NH_4^+

Preprints (www.preprints.org) | NOT PEER-REVIEWED | Posted: 21 August 2020 doi:10.20944/preprints202008.0468.v1

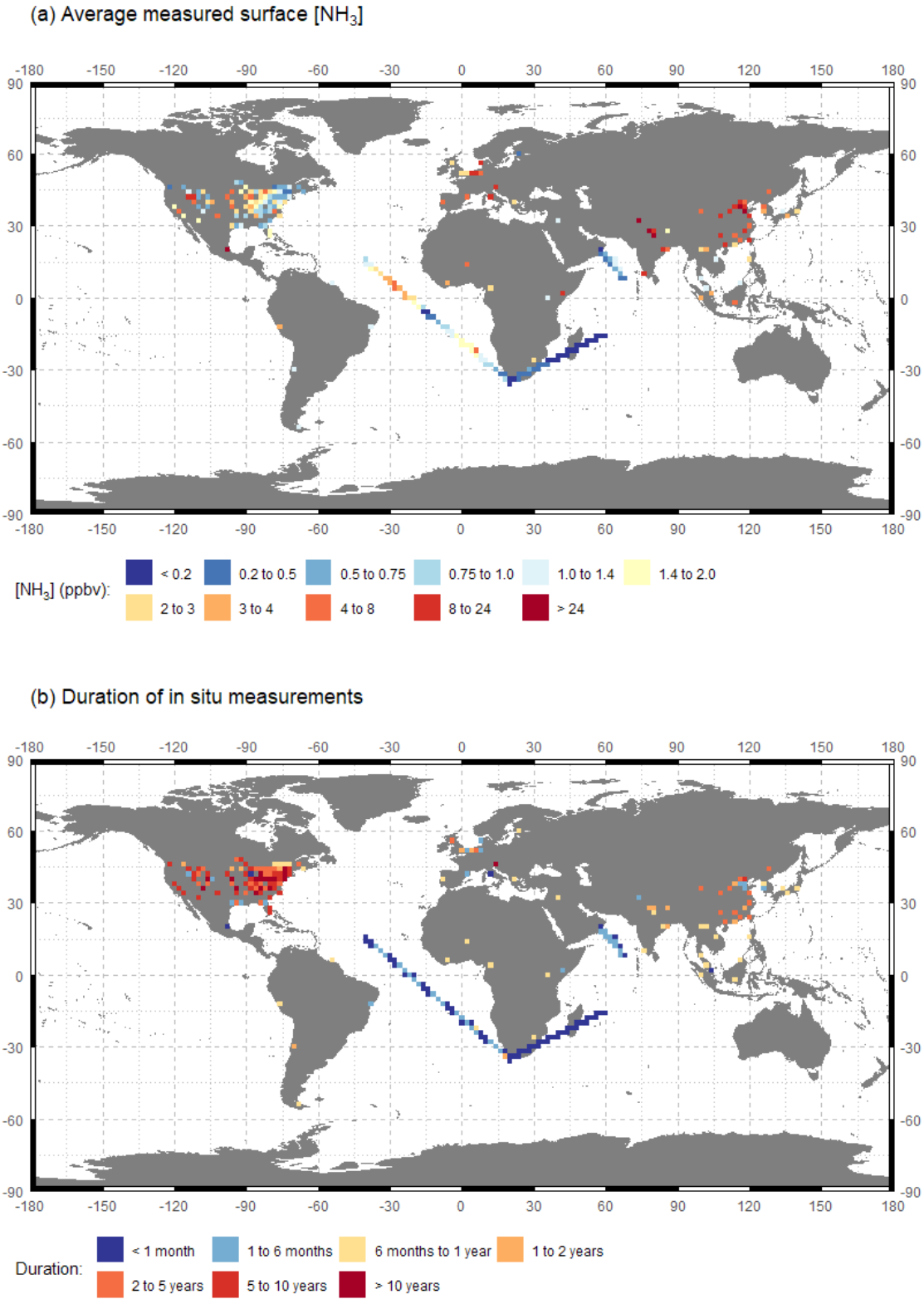

Figure 2. Global in situ measurements reviewed in this paper aggregated to a 1°×1°resolution.

Preprints (www.preprints.org) | NOT PEER-REVIEWED | Posted: 21 August 2020 doi:10.20944/preprints202008.0468.v1

and NH_3 trends and their effects on $PM_{2.5}$ formation. In the US, the Ammonia Monitoring Network (AMoN; 52,53) provides biweekly integrated surface measurements of [NH_3] from a network of 123 sites, with the longest measurement period from October 2007 to present and average measurement duration of 7 years. NH_3 is collected using a passive diffusion sampler and subsequently its laboratory measurement is conducted by sonic dislodgment of NH_4^+ ions from the phosphoric acid sorbent and subsequent Flow Injection Analysis (FIA). In the UK, the National Ammonia Monitoring Network (NAMN) was established in September 1996 and provides monthly integrated surface [NH_3] from a network of 72 active sites. The NAMN uses a combination of an active diffusion denuder method (DELTA samplers: DEnuder for Long Term Atmospheric, 54) and passive samplers (ALPHA: Adapted Low-cost Passive High-Absorption sampler, 55). In the Netherlands, the Dutch National Air Quality Monitoring Network (LML: Landelijk Meetnet Luchtkwaliteit) and the Measuring Ammonia in Nature Network (MAN) have been making measurements of [NH_3] across the Netherlands since 1993 and 2005, respectively. The LML reports hourly [NH_3] since 1993 at 8 sites and since 2014 at 6 sites using continuous-flow denuders (AMORs: Amanda for MOnitoring RIVM; 51) and currently miniDOAS [56], and in two sites, triplets of passive samplers [57] for monthly mean values. While the LML provides high temporal resolution, its low spatial distribution is compensated by over 300 sites of MAN which provide monthly passive sampling measurements of [NH_3]. Apart from these NH_3 monitoring networks, observations of [NH_3] have been made over the ocean in certain campaigns. However, such in situ measurements are significantly fewer compared to those over land. While this has been justified by their distance from human settlements and the order of magnitude less NH_3 over oceans compared to land, recent evidence from Yu *et al.* [5] suggests that NH_3 even in pptv levels can have a significant effect on atmospheric new particle formation.

In the recent years, there have been new methods of instrumentation developed for measurement of [NH_3] with a finer temporal resolution. As seen above, most instrumentation deployed in NH_3 monitoring network has poor temporal resolution, to the extent of biweekly sampling for reduced costs. Additionally, offline analysis may introduce errors due to revolatilization of NH_3 and human errors. Some recent advances that are being implemented or have scope of implementation include: Chemical ionization mass spectrometers (CIMS), QC-TILDAS, Differential optical absorption spectroscopy (DOAS), Monitor for AeRosols and GAses in ambient air (MARGA). Chemical ionization mass spectrometers (CIMS) have been developed for fast time resolution measurement of NH_3 [58–64]. Compared to other emerging instrumentation, the CIMS technique is highly advantageous due to its fast time response (<1 min). However, Nowak *et al.* [60] note that the absolute level and the variability in the instrumental background are a limitation. The Quantum Cascade Tunable Infrared Laser Differential Absorption Spectrometer (QC-TILDAS) determines the mixing ratio of NH_3 by monitoring the molecule's absorption of radiation at 967 cm^{-1} [65]. Differential optical absorption spectroscopy (DOAS) works on the linearization of Lambert-Beer law. With open-path arrangement, DOAS provides a contact-free technique for in situ measurement of [NH_3], within the 203.7–227.8 nm UV wavelength range over path lengths up to 100 m [66–69]. To overcome the issues with instrument performance [70,71], significant improvements have been made over the recent years, mainly by Volten *et al.* [72] and Sintermann *et al.* [73], which improve the reliability as well as reduce the cost of this instrument. The Monitor for AeRosols and GAses in ambient air (MARGA; 74,75) is an online instrument that provides hourly time-resolved measurement of water-soluble gases and aerosols using a dual-channel ion chromatograph. These new developments of in situ [NH_3] measurement techniques are exciting for the insights that can come from continuous and high-resolution data, especially from model–observation comparisons.

For further reading, the reader is directed to some literature on the inter-comparison of these varied techniques [63,64,76–78].

Preprints (www.preprints.org) | NOT PEER-REVIEWED | Posted: 21 August 2020 doi:10.20944/preprints202008.0468.v1

2.2. Satellite remote sensing

Table 1. Some satellite remote sensing studies of atmospheric [NH_3].

Reference	Region	Instrument	Period	Typical concentration
[79]	Beijing	TES	10 Jul 2007	5 to 25 ppbv
[80]	Global	IASI	2008	
[81]	Mediterranean basin	IASI	25 Aug 2007	$5.7\pm0.1\times10^{16}$ molecules cm^{-2}
[82]	Global	IASI	2006 to 2009 (Various)	
[83]	California	IASI	2008	3 to 10 ppbv
[84]	North Carolina	TES	2002	1 to 6 ppbv
[85]	Global	IASI	Apr 2009 to Mar 2010	
[86]	Central Russia	IASI	Jul and Sept 2010	$< 8\times10^{17}$ molecules cm^{-2}
[87]	US	TES	Apr, Jul, and Oct 2006 to 2009	
[88]	Global	IASI	1 Nov 2007 to 31 Oct 2012	$< 10^{17}$ molecules cm^{-2}
[89]	California	TES	16 Jan to 6 Feb 2013	$< 7\times10^{16}$ molecules cm^{-2}
[90]	Global	TES	2007	
[91]	Canadian Oil Sands	TES	August to Sept 2013	
[92]	Central US	CrIS	Jul 2005	
[93]	Global	IASI	2008 to 2013	
[94]	FTIR Stations	IASI	2008 to 2014	
[95]	Global	MIPAS	2003 to 2011	
[96]	Global	AIRS	Sept 2002 to Aug 2015	
[97]	Regional	AIRS	2002 to 2016	
[98]	California	TES	7 May to 3 Jun 2010	21 ± 17 ppbv
[99]	North Africa	IASI	7 May to 3 Jun 2010	$\approx 10^{16}$ molecules cm^{-2}
[100]	Global	IASI	2008 to 2017	
[101]	Canada	IASI & CrIS	May 2016	
[102]	Tanzania	IASI	2008 to 2017	$< 4\times10^{16}$ molecules cm^{-2}
[103]	Global	IASI	2008 to 2017	
[104]	Global	CrIS	2013 to 2017	2 to 10 ppbv
[105]	Global	TANSO-FTS	2009 to 2014	$\approx 10^{16}$ molecules cm^{-2}

Abbreviations– FTIR: Fourier-Transform InfraRed spectroscopy, TES: Tropospheric Emission Spectrometer onboard NASA's Aura satellite, IASI: Infrared Atmospheric Sounding Interferometer onboard the European Space Agency's (ESA) MetOp satellites, CrIS: Cross-track Infrared Sounder onboard NOAA's Suomi NPP satellite, MIPAS: Michelson Interferometer for Passive Atmospheric Sounding onboard ESA's Envisat satellite, AIRS: Atmospheric Infrared Sounder onboard NASA's Aqua satellite, TANSO-FTS: Thermal And Near infrared Sensor for carbon Observations - Fourier Transform Spectrometer onboard JAXA's GOSAT-1.

NH_3 has a remarkable microwave spectrum due to the characteristic "ammonia inversion" [106]. The molecule has a trigonal pyramidal shape with protons on the three points on the base and nitrogen on the top/bottom. This and the fortuitous distance (crossable tunneling barrier) between the protons on the base, allows for nitrogen to pass through the base and change the orientation of the molecule. This causes a strong absorption when microwave/IR photons cause the rapid flipping between the upward pyramidal and downward pyramidal states. Another outcome of the inversion is an inversion doubling, where the infrared spectrum undergoes doubling due to the two possible positions of the nitrogen atoms. Now this opens a whole new avenue for satellite remote sensing of NH_3 in the gas-phase. The unique IR spectrum of NH_3 can make it distinguishable from other chemical species and background noise. With the plethora of infrared spectrometers available in orbit around Earth, providing the possibility of continuous, real-time, global measurement, it was inevitable that this feature of the NH_3 molecule would be tapped into.

The first attempt was when Beer *et al.* [79] used infrared radiances measured by the Tropospheric Emission Spectrometer (TES) onboard the EOS Aura satellite to infer [NH_3] from the spectral residual differences (calculated as per 107) in the region of 960–972 cm^{-1}. This was a demonstration of the possibility of detecting NH_3 from nadir viewing remote sensing instruments. Due to the limitations of the TES — its small geographic coverage and consequent inability to provide daily coverage — attention was shifted to the Infrared Atmospheric Sounding Interferometer (IASI) onboard the MetOp-A satellite. Although this had a poorer spectral resolution than the TES, it provided a broader spatial coverage. Clarisse *et al.* [80] made the first annual "global NH_3 integrated concentrations

Preprints (www.preprints.org) | NOT PEER-REVIEWED | Posted: 21 August 2020 doi:10.20944/preprints202008.0468.v1

retrieved from satellite measurements". Expectedly, there has been a subsequent flurry of activity (see Table 1) in using satellite remote sensing to measure ambient NH_3 in the atmosphere.

Satellite remote sensing is capable of capturing spatiotemporal variations in columns as well as surface NH_3 concentrations [80,84,92,96,105]. For instance, Heald *et al.* [108] found underestimation of NH_3 emissions in the Midwest during spring and in California using IASI data. This was followed by demonstration of potentially constraining NH_3 emissions using TES [NH_3] data [87], with improved modeling of [NH_3] over the US. Thus satellite remote sensing of [NH_3] can also provide constraints towards improvement of NH_3 emission inventory used in chemical transport models.

While satellite-based inference can fill the gaps in observations of [NH_3] and additionally provide its vertical profile, there are limitations associated with this technique as noted in several studies listed in Table 1. Currently deployed instrumentation is not onboard geostationary satellites, and result in a discontinuous temporal measurement. The requirement of a strong thermal contrast reduces reliability of nighttime measurements. The presence of clouds also affects the retrievals. Further, there are issues in the inference of [NH_3] from the radiances measured by the satellite instrument, with a priori assumptions on the [NH_3] profile and shape for conversion of radiances into a concentration. This is further compounded by the small signal of NH_3 in comparison to the background.

To overcome and understand the above issues, validation studies have been carried out. For the TES, NH_3 retrievals were able to capture spatiotemporal patterns observed on the surface by an ammonia monitoring network (CAMNet) in North Carolina [84] and with aircraft measurements [89]. Damme *et al.* [93] demonstrated consistency of IASI NH_3 retrievals with surface NH_3 monitoring networks and aircraft campaigns.

3. Modeling [NH_3]

Atmospheric modeling provides another approach to quantify [NH_3] in the atmosphere. Considering NH_3, models can (1) evaluate the environmental impacts of their emissions and depositions, (2) help project the impact of future scenarios, (3) aid in developing our understanding of the processes controlling atmospheric [NH_3], (4) examine the role of NH_3 in affecting atmospheric chemical and physical processes, and (5) study aerosol formation (both mass and number concentrations) dependent on [NH_3].

The first modeled global distributions of [NH_3] were derived by Dentener and Crutzen [169] with their development of an NH_3 emission inventory incorporated into a climatological three-dimensional global tropospheric transport model (MOGUNTIA; 170). This was a first attempt at understanding the fate of reduced nitrogen species in the atmosphere. A $10° \times 10°$ NH_3 emission inventory was used in this initial modeling study. Subsequently, there has been vigorous development in the modeling of [NH_3], with two approaches: Eulerian (Table 2) and Lagrangian (Table 3). The more typical implementation is the Eulerian approach (in GEOS-Chem, CMAQ, and EMEP among others), where the properties of reference grid cells are monitored. The Lagrangian approach, which "follows" the air parcel, is applied in models such as FRAME, TREND, and STILT-CHEM.

GEOS-Chem (www.geos-chem.org) is one of the most widely used (see Table 2) three-dimensional chemical transport models (3-D CTM) in the study of NH_3 in the atmosphere. Due to the environmental policies in Europe, there are several implementations for the region – TM5 [132], EMEP model [115,116, 171], Danish Ammonia Modeling System (DAMOS)/Danish Eulerian Hemispheric Model (DEHM) [113,114,134], CHIMERE [109], MATCH [126] and LOTUS-EUROS [172]. The Community Multiscale Air Quality Modeling System (CMAQ) [173] while commonly used for air quality studies, especially over North America, is not widely [111] used to understand [NH_3]. Particulate Matter Comprehensive Air Quality Model with Extensions (PMCAMx) [128–130] has also been utilized for modeling NH_3 over the US [127] and Europe [131]. Unlike these Eulerian CTMs, the Lagrangian approach in modeling atmospheric NH_3 is used in the following – TERN [166], TREND model [167,168], ACDEP [133–139], Fine Resolution AMmonia Exchange (FRAME) [153,155,156], NAME model [158], and A Unified Regional Air-quality Modeling System (AURAMS) [141], Operational Priority Substances (OPS) [161–

Preprints (www.preprints.org) | NOT PEER-REVIEWED | Posted: 21 August 2020 doi:10.20944/preprints202008.0468.v1

Table 2. Some modeling studies of atmospheric [NH_3] using Eulerian chemical transport models.

CTM	Equilibrium Model	Reference	Region	Period
CHIMERE	ISORROPIA	De Meij *et al.* [109]	Northern Italy	2005
CMAQ	MARS-A	Gilliland *et al.* [110]	Eastern US	2001
CMAQ	MARS-A	Gilliland *et al.* [111]	US	2001
DAMOS	Frohn [112]	Brandt *et al.* [113]	Europe, North America	
DAMOS	Frohn [112]	Geels *et al.* [114]	Denmark	2007
EMEP	EQSAM	Fagerli and Aas [115]	Europe	1990–2003
EMEP	EQSAM	Horvath *et al.* [116]	Hungary	1990 and 1995–2004
GEOS-Chem	ISORROPIA II	Heald *et al.* [108]	US	May 2009 to April 2010
	ISORROPIA II	Walker *et al.* [117]	California	2009
	RPMARES	Zhang *et al.* [118]	US	2006 to 2008
	ISORROPIA II	Schiferl *et al.* [34]	California	May and Jun 2010
	ISORROPIA II	Paulot *et al.* [119]	Global oceanic	1995–2004
	RPMARES	Luo *et al.* [90]	Global	2007
	MARS-A	Zhu *et al.* [120]	Global and US	2008
	ISORROPIA II	Schiferl *et al.* [121]	US	2008–2012
	ISORROPIA II	Yu *et al.* [122]	US	2001–2016
	ISORROPIA II	Nair *et al.* [123]	US	2001–2017
GEOS-Chem (adjoint)	ISORROPIA/MARS-A	Zhu *et al.* [87]	USA	Apr, Jul, and Oct 2006–2009
	RPMARES	Paulot *et al.* [124]	US, E.U., China	2005–2008
LOTOS-EUROS	CBM-IV	van Damme *et al.* [125]	Europe	2008–2011
MATCH		Langner *et al.* [126]	Baltic Sea Basin	1996–2001
PMCAM$_x$	ISORROPIA	Pinder *et al.* [127]	USA	Jul and Oct 2001, Jan and Apr 2002
		Murphy and Pandis [128]	Eastern US	Jul 2001
		Tsimpidi *et al.* [129]	Mexico City	Apr 2003
		Karydis *et al.* [130]	Mexico City	Apr 2003
		Fountoukis *et al.* [131]	Europe	May 2008
TM5	EQSAM	de Meij *et al.* [132]	Europe	2000

See Table S2 for details of Equilibrium Models. *Abbreviations*– CTM: Chemical Transport Model, CHIMERE:, CMAQ: Community Multiscale Air Quality, DAMOS: Danish Ammonia MOdeling System, EMEP: European Monitoring and Evaluation Programme, GEOS-Chem: Goddard Earth Observing System - Chemistry, LOTOS-EUROS: LOngTerm Ozone Simulation - EURopean Operational Smog, MATCH:, PMCAM$_x$:, TM5: Tracer Model 5.

Preprints (www.preprints.org) | NOT PEER-REVIEWED | Posted: 21 August 2020 doi:10.20944/preprints202008.0468.v1

Table 3. Some modeling studies of atmospheric [NH_3] using Lagrangian chemical transport models.

CTM	Equilibrium Model	Reference	Region	Period
ACDEP	Modified CBM-IV	Hertel *et al.* [133]	Denmark	1990
		Hertel *et al.* [134]	Baltic Sea	1999
		Gyldenkaerne *et al.* [135]	Northwestern Europe	1999–2001
		de Leeuw *et al.* [136]	North Sea	1999
		Skjøth *et al.* [137]	Denmark	1998 and 1998
		Skjøth *et al.* [138]	Denmark	1999 to 2001
		Skjøth *et al.* [139]	Europe	2007
AURAMS	Makar *et al.* [140]	Makar *et al.* [141]	North America	2002
FRAME	Barrett *et al.* [142]	Fournier *et al.* [143]	British Isles	1996
		Fournier *et al.* [144]	British Isles	1996
		Fournier *et al.* [145]	UK	1996
		Dore *et al.* [146]	UK	2002
		Sutton *et al.* [147]	UK	2002–2004
		Tang *et al.* [148]	UK	2012
		Vieno [149]	UK	1999
		Sutton *et al.* [150]	UK	Sep 1996 to Nov 2000
		Sutton *et al.* [151]	UK	1996
		Hellsten *et al.* [152]	UK	2000
		Singles *et al.* [153]	Great Britain	1987 to 1990
		Hallsworth *et al.* [154]	UK	2002–2004
		Kryza *et al.* [155]	Poland	2002–2005
		Zhang *et al.* [156]	North China Plain	2008
NAME	Meng and Seinfeld [157]	Redington and Derwent [158]	UK	1996
OPS		van Pul *et al.* [159]	Netherlands	Sep 2000 to 2001
		van Jaarsveld [160]	Netherlands	Jan 1998 to Dec 2000
		van Pul *et al.* [161]	Eastern Netherlands	2002–2003
		Stolk *et al.* [162]	Netherlands	2005–2007
		van Pul *et al.* [161]	Netherlands	Jul 2002 – Aug 2003
		Kruit *et al.* [163]	Netherlands	1990–2014
		van der Swaluw *et al.* [164]	Netherlands	1998–2002
STILT-Chem	Wen *et al.* [165]	Wen *et al.* [165]	Canada	Jun to Nov 2006
TERN		ApSimon *et al.* [166]	UK	1983
TREND		Asman and van Jaarsveld [167]	Europe	1990
		Asman [168]	Denmark	1996

Abbreviations– CTM: Chemical Transport Model, ACDEP: Atmospheric Chemistry and DEPosition, AURAMS: A Unified Regional Air quality Modeling System, FRAME: Fine Resolution AMmonia Exchange, NAME: Nuclear Accident ModEl, OPS: Operational Priority Substances, STILT-Chem: Stochastic Time-Inverted Lagrangian Transport and Chemistry, TERN: Transport over Europe of Reduced Nitrogen.

Preprints (www.preprints.org) | NOT PEER-REVIEWED | Posted: 21 August 2020 doi:10.20944/preprints202008.0468.v1

163] and STILT-Chem [165]. Some of the significant modeling studies of atmospheric NH_3 using these various models are enumerated in Tables 2 and 3. The following three subsections detail the three most important processes to be considered in the modeling of NH_3, viz. emission, gas-particle partitioning, and deposition.

3.1. Emission

Emission inventories are required for representation in chemical transport models (CTMs), in addition to utility for assessment of air quality policies. They have been developed on scales ranging from global to regional to local for use in CTMs. Global NH_3 emission inventories include the Community Emissions Data System (CEDS; 174), the Emissions Database for Global Atmospheric Research (EDGAR; 175), MASAGE_NH_3 [124], and the Global Emissions Inventory Activity (GEIA; 18). Examples of regional NH_3 emission inventories are the US EPA/NEI (National Emission Inventory; https://www.epa.gov/air-emissions-inventories), Canada's APEI (Air Pollutant Emissions Inventory; 176), EMEP (European Monitoring and Evaluation Programme) WebDab (https://www.ceip.at/webdab-emission-database/reported-emissiondata), NAEI (National Atmospheric Emission Inventory) for the UK [177], NEMA (National Emission Model for Ammonia; 178) for Netherlands, Asian MIX inventory [179], Regional Emission inventory in ASia (REAS) [180–185], and DICE-Africa (Diffuse and Inefficient Combustion Emissions in Africa; 186). There are inventories developed with higher spatial resolution for the Eastern United States [110], North Carolina and the San Joaquin Valley [187], and the Pearl River Delta [188] and Yangtze River Delta [189] in China.

NH_3 emissions are primarily anthropogenic, coming mainly from agriculture through excreta from domestic animals and use of synthetic fertilizers [190–196]. Approximately 60% of total NH_3 emissions are from anthropogenic sources [18,197], of which 80–90% are from agricultural activity (fertilizers and livestock wastes) [18,187,190,198]. Other sources of NH_3 include fuel combustion from vehicles and industries, biomass burning, and human wastes. Emission inventories are, therefore, generally based on emission factors from a particular source type and associated activity rate. Emission factors are based on measurement of NH_3 fluxes from individual source types such as animal houses and storage, fertilizer application, fuel combustion, biomass burning, human wastes, industries, transportation, vegetation, and soil. Activity factors indicate the potential emission from each source for specific locations based on parameters like the amount of livestock, the amount of fertilizer applied, the amount of fuel combusted, etc. based on the source type. Product of the source-specific emission factor with the activity factor generates the estimated spatial distribution of NH_3 emissions, i.e. the emission inventory.

The main issues with the development of reliable NH_3 emissions inventories are the dearth of emission measurements, incomplete identification of all known sources of emissions, the lack of validation with [NH_3] measurements, variability and uncertainty of emissions estimates dependent on free ammonia concentration, and differences in inventory compilation approaches due to assumptions regarding underlying emission factors and activity rates, and source significance influenced by spatial scales [127,177,187]. While the bottom–up approach of emissions inventory is expected to be accurate due to detailed consideration of each source type and their emissions, it requires comprehensive information for activity factors to apply emission factors. This would require detailed measurements to capture the complex spatial variability of emissions across source types as well as temporal variability (as discussed in Section 5). Gilliland *et al.* [110,111] and Pinder *et al.* [127] observed erroneous seasonal variations in model simulated ammonium and reduced nitrogen. Zhang *et al.* [118] determined NH_3 emissions (constrained and scaled by observations) are a factor of 3 lower in winter than summer and in better agreement with US network measurements of NH_x (NH_3 + NH_4^+) and NH_4^+ wet deposition fluxes. Applying the modifications seemed to correct the previous observations. The underestimation of NH_3 emissions in models was confirmed further by Walker *et al.* [117], with the additional under-prediction of HNO_3 contributing to under-prediction of nitrate over California.

Preprints (www.preprints.org) | NOT PEER-REVIEWED | Posted: 21 August 2020 doi:10.20944/preprints202008.0468.v1

Recently, top–down approaches have been shown to reduce the identified issues with the accuracy of NH_3 emissions inventories by inverse modeling to relate observed [NH_3] to model emissions [87,108,110,111,117,124,127,199]. Although these studies have to grapple with the complexities of other model processes, comparison with bottom–up emission inventories can identify improvements in NH_3 source identification and contribution. Another approach towards improving emissions inventories are using a combination of bottom–up and top–down approaches in a "hybrid" approach [138,200]. Regardless, current emission inventories have enabled high-resolution chemical transport models to generally capture spatial variability of atmospheric NH_3 and NH_4^+ concentrations and provide a wealth of information that is currently unobtainable from direct observations, while also improving understanding of the effects of various processes and parameters in determining [NH_3].

3.2. Gas-particle partitioning

Another significant aspect of modeling atmospheric [NH_3] is the accurate capture of phase partitioning. This is achieved through either thermodynamic equilibrium schemes or explicit mass transfer dynamical schemes. Thermodynamic equilibrium schemes generally assume aerosols to be internally mixed, i.e. all aerosol particles of certain size range have the same composition. They also generally assume thermodynamic equilibrium in gas-particle partitioning of volatile chemical species. These approaches trade-off accuracy (former) versus computational resources (latter). Some balance can be achieved with assuming the volatile constituents being in equilibrium and shifting to mass transfer schemes when this assumption is not valid in conditions resulting in a longer chemical equilibration time as compared to the gas-aerosol diffusion timescale, typically cooler conditions.

Over the last four decades, there has been steady development in this aspect. EQUIL was developed by Bassett and Seinfeld [201] to calculate the aerosol composition of the NH_4^+–SO_4^{2-}–NO_3^-–H_2O aerosol system. KEQUIL was their [202] improvement of EQUIL with the incorporation of Kelvin Effect. Saxena *et al.* [29] developed the MARS scheme for the SO_4^{2-}–NO_3^-–NH_4^+–H_2O system with reduced computational time through sub-domains based on RH and NH_3:SO_4^{2-} for aerosol species to reduce number of equations. Further improvements were made by Binkowski and Shankar [203] and Binkowski and Roselle [204]. SEQUILIB by Pilinis and Seinfeld [205] considered Na and Cl, heretofore ignored, but important for marine aerosols. Kim *et al.* [206] developed a computationally efficient gas-aerosol equilibrium model SCAPE (Simulating Composition of Atmospheric Particles at Equilibrium) without limiting assumptions. AIM [207] and AIM2 [208] approached the problem by direct minimization of the Gibbs free energy. The absence of approximations on the equilibrium concentration made AIM computationally intensive. GFEMN [209] was another iterative Gibbs free energy minimization method.

A significant step forward towards improved computational efficiency was achieved by Nenes *et al.* [210] with the development of ISORROPIA. ISORROPIA examined the Na^+–NH_4^+–Cl^-–SO_4^{2-}–NO_3^-–H_2O aerosol system using pre-calculated lookup tables and a single level of iteration to make this scheme computationally efficient. This was further developed by Fountoukis and Nenes [211] into ISORROPIA II, which treats the K^+–Ca^{2+}–Mg^{2+}–NH_4^+–Na^+–SO_4^{2-}–NO_3^-–Cl^-–H_2O aerosol system, i.e. added crustals. ISORROPIA II is currently the most used thermodynamic equilibrium module within GEOS-Chem. A contrasting effort aimed at accuracy over speed is EQUISOLV [212], where direct numerical computation without simplifying assumptions was used to obtain equilibrium concentration. The three levels of nested iteration loops for higher order reactions made this computationally expensive. This was further developed into EQUISOLV II [213] with the replacement of the mass-flux iteration (MFI) method with the analytical equilibrium iteration (AEI) method for solving the set of equilibrium equations. Further, the scheme was expanded to consider the potassium, calcium, magnesium, and carbonate systems. Development of thermodynamic equilibrium schemes has not been stagnant, with recent examples including HETV [140], MESA [214], ADDEM [215], and UHAERO [216]. The multicomponent equilibrium solver for aerosols (MESA) appears most interesting, with the use of a computationally

Preprints (www.preprints.org) | NOT PEER-REVIEWED | Posted: 21 August 2020 doi:10.20944/preprints202008.0468.v1

efficient modified pseudo-transient continuation technique for solving the set of equilibrium reactions while maintaining overall accuracy. For a detailed review and comparison of thermodynamic equilibrium schemes, we direct you to the works of Kim *et al.* [206], Amundson *et al.* [216], Pilinis [217], Zhang *et al.* [218].

The assumption of equilibrium may not be justified under certain conditions, which then require explicit mass transfer dynamical schemes for gas-particle partitioning. While the equilibrium assumptions are not there to affect the accuracy of solution, the computational cost hinders the use of these mass transfer schemes within CTMs. Development in this aspect has been limited compared to thermodynamic equilibrium schemes, with work by Meng and Seinfeld [157], Jacobson *et al.* [212], Jacobson [219,220], Meng *et al.* [221], Sun and Wexler [222], Pilinis *et al.* [223]. Hybrid methods have recently been developed, where the condensation or evaporation of aerosol particles with diameters less than a threshold (≈ 1 μm) are simulated using thermodynamic equilibrium schemes, and the dynamic mass-transfer approach is used for the larger particles [224–227].

3.3. Deposition and Bi-directional exchange

Atmospheric ammonia is deposited to the surface in either the gaseous (NH_3) or aerosol (NH_4^+) form. Unionized NH_3 is mainly transferred out of the atmosphere to the surface through dry deposition [118,228]. Dry deposition of NH_3 is faster than that of NH_4^+ by a factor of 10–100, depending on [NH_3], plant/terrain, and diurnal variations with meteorological conditions [229]. This leads to a short atmospheric lifetime for NH_3 leading to significant deposition near its sources due to the fast deposition and higher concentration [230,231].

Representation of deposition of NH_3 in models is difficult due to the dearth of its measurements and because this is a complex process. Dry deposition can be typically separated into that onto soil and that onto vegetation. This process is dependent on [NH_3] above the particular surface, the equilibrium [NH_3] over the surface determining whether emission or deposition occurs, turbulence over the surface, and extent of moisture. Studies, such as Langford and Fehsenfeld [232], show that bi-directional exchange of NH_3 over vegetation is an important process, which still does not find adequate representation in models. Even this process is further complicated in that the mechanism for vegetation as a sink of NH_3 could be either through cuticular or stomatal uptake [229,233]. Sutton *et al.* [234] identify that accurate model representation of bi-directional exchange of NH_3 is important for models to accurately quantify [NH_3], with implications for its deposition, emission, re-volatilization, and lifetime.

Although Sutton *et al.* [235] and Nemitz *et al.* [236] developed the first models for bi-directional surface–atmosphere exchange of NH_3, chemical transport models neglected to incorporate these until over a decade later. These studies [237–240] have shown better model–observation agreements resulting in more accurate quantification of [NH_3]. However, some more recent studies highlight that consideration of bi-directional exchange alone may not be sufficient. While Zhu *et al.* [120] implemented bidirectional exchange of NH_3 into their GEOS-Chem simulations and observed improved agreement of model simulated [NH_3] with network (AMoN) measurements, the general large underestimates (2–5 times) were not corrected, reiterating the need for accurate representation of emissions. In contrast to the results of Heald *et al.* [108] for the San Joaquin valley, Zhu *et al.* [120] also demonstrated that adjustment to HNO_3 does not significantly affect simulated [NH_3] over AMoN sites. This is consistent with Park [241], which suggests nitrate formation is NH_3-limited over most of the United States. Incorporation of bi-directional exchange of NH_3 did not resolve the model overestimation (3–5 times) of nitrate. Recent work by Luo *et al.* [242,243] shows that applying an improved wet scavenging parameterization in GEOS-Chem reduces the overestimation of nitrate and nitric acid in the model and corrects some of the deviations in atmospheric NH_3 concentrations.

Preprints (www.preprints.org) | NOT PEER-REVIEWED | Posted: 21 August 2020 doi:10.20944/preprints202008.0468.v1

3.4. Model–Observation comparisons

Validation of model simulated [NH_3] with real measurements is the most important exercise not merely for the justification of model output, but for further model refinement and development.

Heald *et al.* [108] examined GEOS-Chem simulated [NH_3] with ground (IMPROVE) and satellite (IASI) measurements. The study demonstrated that emissions were underestimated in California and in the Midwest, which was the likely reason for the underestimation of NO_3^- formation in GEOS-Chem. This was further confirmed by Walker *et al.* [117] with the added possibility of HNO_3 underestimate and topography effects on mixed layer depths. Both studies showed that GEOS-Chem underestimated [NH_3] compared to satellite and in situ measurements.

Schiferl *et al.* [121] showed the mean modeled [NH_3] was underestimated (2.5 ppbv vs. observed 3.4 ppbv) over the US during summer through comparison with measurements from 2008 to 2012 at 11 AMoN sites. During summer, the range in model-simulated [NH_3] was smaller, and its mean was lower (by more than 25%) when compared to AMoN measurement data. Schiferl *et al.* [121] suggests that this may not be model deficiency, but that the AMoN sites' location near high NH_3 source regions, causes a sampling bias due to inadequate representation of the range of [NH_3] across the US. Although modeled [NH_3] was underestimated during summer, especially near source regions (including both agricultural and fire emissions), it showed consistency in spatiotemporal variability of [NH_3] in the column and at the surface. Inter-annual variability of modeled surface [NH_3] was lower than measurements, but the trends and variability are significant considering the fixed NH_3 emissions in the model.

Paulot *et al.* [124] optimized simulated seasonality and magnitude of [NH_3] in the Northeast and Southwest US using the adjoint of GEOS-Chem by inversion of NH_4^+ wet deposition fluxes from NADP network data for the period 2005–2008. They developed a novel bottom-up emission inventory (MASAGE_NH_3), which simulated the magnitude and seasonality of [NH_3] in better agreement with observations in Northeast and Southeast US, consistent with NH_3 emissions overestimate in the US National Emissions Inventory. In Midwest and upper Midwest, spring enhancement in NH_3 is captured but not the elevated summer concentrations. Underestimation is still significant in Atlantic and Central regions, especially in winter in the Central US.

US NH_3 sources are constrained using TES satellite observations with the GEOS-Chem model and its adjoint by Zhu *et al.* [87]. There is an improvement in the underestimation of NH_3. The range and variability improved in April and October with reduced model underestimates, however with overestimation in July due to the constraints applied. Zhu *et al.* [120] tries further improvements by incorporating a bi-directional exchange (BIDI) scheme for NH_3, which improves the normalized mean bias. Large underestimation (especially in October and April) still exist, which is likely due to the significant errors in NH_3 emission inventories.

Yu *et al.* [122] and Nair *et al.* [123] comprehensively assessed long-term (last 2 decades) GEOS-Chem simulated [NH_3] over United States with empirical measurements. The strong dependence on emissions for seasonality and on acid precursor gases for long-term trend are demonstrated. Potential improvements in the representation of emissions especially over the US Great Plains region are identified. Further, their results indicate that modeled [NH_3] is more strongly dependent on NH_3 emissions than observations are. Additionally, especially over Southeast US, considerations of changing acid precursor gas concentrations or particle acidity may need to be made in modeling NH_3.

4. Spatial distributions

[NH_3] is predominantly controlled by emissions due to the short atmospheric lifetime of NH_3. Transport, obviously, plays a role especially that of particulate ammonium that re-volatilizes into the gas phase NH_3. The main source of NH_3 emissions is agricultural land especially in the period after chemical fertilizer application. Consequently, most NH_3 hotspots are over these regions of agriculture.

Preprints (www.preprints.org) | NOT PEER-REVIEWED | Posted: 21 August 2020 doi:10.20944/preprints202008.0468.v1

Putting together the vast literature of surface measurements of [NH_3] shows their spatial distribution and hotspots (Figure 2). Over the US, highest surface [NH_3] is observed in the Midwest and California. This is due to agriculture (including concentrated animal feeding operations) and biomass burning. Similar reasons explain the observed hotspots of NH_3 over Europe and the North China Plain. The recent use of satellite remote sensing to quantify [NH_3] has the advantage of directly providing a global picture. Clarisse *et al.* [80] provided the first such global NH_3 map using data from the IASI/MetOp satellite for the year 2008. Their results confirm global NH_3 hotspots (total column $NH_3 > 0.5\ ^{-}g\,m^{-2}$) over agricultural valleys and regions of biomass burning. Using 5 years of IASI measurements, van Damme M. *et al.* [244] provided a more detailed global map. Agricultural hotspots were identified over the Indo-Gangetic plain, North China Plain, and other highly irrigated regions in Asia. Over Indonesia, there was the combined effect of intensive fertilizer application in Java and wildfires in Borneo and Sumatra. Over South America, hotspots were mainly due to biomass burning, but new agricultural hotspots over Chile and Colombia-Venezuela were revealed. Over North America, [NH_3] was elevated over the Midwest US and the San Joaquin Valley. Anthropogenic NH_3 effects were seen in parts of Canada as well. Over Europe, hotspots were over Netherlands and the Po Valley, Italy. The effect of industrial emissions was captured over South Africa. Over these hotspots, measurements would exceed total column NH_3 of 3×10^{16} molecules cm^{-2}. Using the TES data for the year 2007, Luo *et al.* [90] showed the enhancement of NH_3 over Northern India (up to 14.45 ppbv NH_3 in the summer) and North-Central China and spring biomass burning effects in parts of Africa and Asia. Warner *et al.* [96] provided a 13-year record of global NH_3 distribution that confirmed the importance of agriculture and biomass burning in determining the hotspots over these regions.

Agricultural land is often mixed-use, with livestock rearing, which further contributes to NH_3 emissions. Xing *et al.* [245] indicated that NH_3 emissions from livestock activities have increased by 11% from 1990 to 2011 in USA. This could have effects on the spatial distribution of [NH_3]. Li *et al.* [246] found large spatial differences in [NH_3] over the northeastern plains of Colorado, a region of concentrated agricultural activities and animal feeding operations, with mean NH_3 concentrations ranging from 4–60 ppbv from grasslands to feedlots with almost 100k cattle. Over USA, data from measurements and modeling [122,123] indicate spatial heterogeneity based on land-use. The Midwest shows the highest concentrations of NH_3 due to the intensive agricultural activities (including livestock rearing) as well as the energy sector. In the eastern part of USA, NH_3 in the gas-phase is limited due to the elevated SO_2 and NO_x emissions from the coal-fired power plants as well as manufacturing in the Ohio River Valley region. In the western part of USA, [NH_3] are elevated over the San Joaquin Valley possibly due to biomass burning and agriculture. Their study indicates that hotspots are highly NH_3 emission dependent and cold spots are highly SO_2 and NO_x emission dependent.

China is a large agricultural nation contributing approximately 20% of global NH_3 emission [180,182,183]. Roughly 20% of the world population is fed by 10% of Earth's arable land, requiring intensive agriculture and livestock rearing. The concentrated use of fertilizers (30% of global usage; http://www.stats.gov.cn/) as well as livestock wastes contribute significantly to the NH_3 emission [247,248]. Meanwhile, chemical fertilizer application in China is less efficient to keep costs down, resulting in a high degree of nitrogen loss (NO^-, NH_3, N_2O, and N_2). Further, about 30% of livestock products originate from the North China Plain (NCP), which further increases the NH_3 emission in this highly polluted region. Over China, Liu *et al.* [249] used IASI satellite NH_3 NH_3 retrievals and vertical NH_3 profiles from MOZART to provide a comprehensive estimate of surface [NH_3] over the region. The spatial distribution of [NH_3] was as expected, aligned with the intensive agricultural areas. The deviations from this distribution were explainable by concentrated animal farming locations, where livestock wastes contributed more than fertilizer use on farms. NH_3 emission mitigation was not a focus for the nation until 2015, when an NH_3 monitoring network (AMoN-China) was established. Using this network data, Pan *et al.* [250] identify the NCP having highest [NH_3] followed by smaller hotpots over the Tarim basin, Chengdu Plain, and Guanzhong Plain coinciding with intensive agricultural activity.

Preprints (www.preprints.org) | NOT PEER-REVIEWED | Posted: 21 August 2020 doi:10.20944/preprints202008.0468.v1

5. Temporal trends

The concentration of NH_3 in the atmosphere is mainly determined by its emission. Emission is highly human activity and temperature dependent. It is expected then that the temporal trends of NH_3 would be strongly correlated to that of human activity and temperature. We discuss the trends in $[NH_3]$ at the different temporal scales.

5.1. Diurnal

Diurnal variation in ambient $[NH_3]$ has been observed to varying degrees. Variation in temperature is the primary reason for this. It may mainly affect local emissions, which are temperature dependent and may also modulate the boundary layer depth and consequently the concentrations at the surface. Additionally, gas-particle partitioning generally peaks in the afternoon. Thus the NH_3 mixing ratios are typically at a minimum in the early morning, peak near midday, and decrease during the night [e.g., 251]. On the flip side, Alkezweeny *et al.* [252] were among the earliest to demonstrate lower daytime $[NH_3]$ as nighttime shows shallower boundary layer depth. Erisman *et al.* [253] lent further evidence of this by observing a strong decrease in $[NH_3]$ with height, which was steeper at night likely due to temperature inversions preventing the upward transport of NH_3.

Delving into this discrepancy, Buijsman *et al.* [254] were able to identify the expected diurnal variation occurring in low NH_3 emission sites and the atypical elevated nighttime concentrations over high emission areas. The relatively lower daytime $[NH_3]$ in high emission areas was due to higher wind speeds and more favorable mixing conditions, while at night there would be accumulation in a shallower boundary layer. For background stations, the opposite observations was due to transport of NH_3 from emission areas; nighttime removal of NH_3 through dry deposition and conversion exceeded the transport contribution. During daytime, $[NH_3]$ increased as atmospheric conditions permitted vertical transport of tropospheric NH_3. Additionally, the difference in $[NH_3]$ between day and night is larger during spring and summer [255], suggesting the influence of higher emissions during warmer months. No clear diurnal profile of $[NH_3]$ was observed in a study by Parmar *et al.* [256] for different seasons in an urban area with elevated $[NH_3]$. Early morning decrease in $[NH_3]$ was attributed to dew formation, which is a significant sink for soluble gases [257].

Perrino *et al.* [258] noted that NH_3 in an urban location is much higher than a nearby rural location and higher than an urban background station with no vehicular traffic. Also, the concentration and temporal trend of NH_3 and CO are well correlated, indicating NH_3 may originate from vehicular emissions and its concentration is dependent on the mixing in the atmosphere. Measurements by Ianniello *et al.* [259] in Beijing, China showed no observed diurnal variability for $[NH_3]$ in both summer and winter. Highest $[NH_3]$ were observed in the early morning during summer ($\sim$150 ppbv) when atmospheric conditions were stable. The diurnal trends of $[NH_3]$ were weakly dependent on air temperature and were affected by wind direction, indicating influence of local and regional sources. $[NH_3]$ showed correlation with boundary layer mixing and with $[NO_x]$, [CO] and $PM_{2.5}$, supporting their hypothesis that vehicular traffic may be a significant NH_3 source in Beijing. Similarly, Gong *et al.* [260] uncovered the contribution of vehicular emissions to the morning rise in the diurnal profile of NH_3 mixing ratios only in winter over urban and suburban areas of Texas, US. Notable spikes were likely due to transport from a coal power plant and some other possible sources. Large differences in NH_3 diurnal profiles between weekday–weekend were likely due to higher weekday industrial activities. Road traffic was also identified by Pandolfi *et al.* [261] as a significant source of NH_3, with a typical bimodal-traffic-driven NH_3 diurnal cycle at an urban site. Significant lowering of mixing height during nighttime in an urban area may lead to higher measured $[NH_3]$ during nighttime [262]. Some trends due to daytime increase in transportation were also observed.

Wang *et al.* [263] observed the diurnal profile of $[NH_3]$ in the urban atmosphere over Shanghai, China to demonstrate a typical bimodal cycle. The two modes occurred during morning and evening traffic emissions and were modulated by atmospheric boundary layer development. On the contrary, atmospheric NH_3 at a rural site showed a single mode (late morning), primarily due to the volatilization

Preprints (www.preprints.org) | NOT PEER-REVIEWED | Posted: 21 August 2020 doi:10.20944/preprints202008.0468.v1

from agricultural emissions as temperatures increased. In an industrial area, the diurnal profile of [NH_3] was irregular and showed no bimodal or unimodal pattern due to large industrial emission pulses, which were variable and mainly during nighttime.

As evinced by the literature reviewed, the diurnal variation in [NH_3] is not so straightforward. Conventional wisdom leads to the expectation of a diurnal profile of NH_3 increasing from dawn till afternoon and then decreasing due to the effect of temperature on emissions. There may be many other factors at play such as transport, boundary layer height, deposition, fertilizer application time, traffic emissions and the interplay of all of these that result in unexpected or even opposite diurnal profiles of NH_3.

5.2. Seasonal

The numerous studies in Table S1 show maximum (minimum) [NH_3] occurring during warm (cold) months. The seasonal cycle in [NH_3] is predominantly a result of the temperature dependence of: (1) gas-particle partitioning between NH_3 and NH_4^+, (2) NH_3 emissions from vegetation, organic wastes, and fertilizers due to Henry's law equilibrium between aqueous- and gas-phase NH_3 [190,264], (3) turbulence, and (4) humidity [265].

Most of the observations listed show the expected maximum of gas-phase [NH_3] in the warmest summer months. Robarge *et al.* [266] examined the various meteorological factors that could affect [NH_3], viz. air temperature, relative humidity, and wind speed and direction. They determined temperature to be the most significant meteorological parameter that determines [NH_3]. Bari *et al.* [267] also demonstrated that the Manhattan summer to winter ratio was 1.5. Anatolaki and Tsitouridou [268] observed [NH_3] were slightly higher during the warm months in Greece. Usually, this is explained by the shift of gas-particle partitioning equilibrium from NH_4NO_3 towards HNO_3 and NH_3 at high temperatures [269]. However, in the conditions at their measurement site, particulate NH_4NO_3 was only expected in the cold period. They suggest that photochemistry for nitric acid and local NH_3 emissions from a fertilizer factory or agricultural activities could explain higher [NH_3]. This is indicative of the potential of factors other than temperature, most importantly the presence of local sources, to play a role in determining the apparent seasonal variation of [NH_3].

An important non-meteorological factor is the application of fertilizers for agriculture, especially in the spring. Hoell *et al.* [270] were among the earliest to identify enhanced NH_3 levels in March possibly due to NH_4NO_3 volatilization from fertilizer. This springtime application of fertilizer may cause deviation from the ammonium nitrate equilibrium constant due to local sources and non-equilibrium conditions caused by high RH and presence of sulfate acid aerosol as observed by Cadle *et al.* [271].

However, Burkhardt *et al.* [272], noted that local sources could possibly explain the maximum seasonal arithmetic mean [NH_3] in spring and autumn, but the seasonal geometric mean [NH_3] were largest in summer. Measurement of [NH_3] is generally reported as arithmetic mean, which is affected to a higher degree by spikes associated with local sources, wheras the geometric mean is more effective at representing background [NH_3]. Thus, summertime [NH_3] is in reality larger than spring and autumn values, where spikes associated with local agricultural emission sources appear to elevate the background [NH_3].

Alebic-Juretic (2008) showed that in a residential area, within a cultivated garden, the seasonal maxima in [NH_3] are obtained during the warmer months of spring and summer. However, near industrial sources, higher [NH_3] is seen in winter and autumn. This is indicative of the role of the boundary layer depth in the highly NH_3 background industrial source region and the role of emissions from the green space in the lower NH_3 background residential region.

These numerous studies and others in Table S1 demonstrate that seasonal variation of NH_3 is as expected along the variation of temperature. It is most concentrated in the summer months and decreases as it gets colder. There may, however, be the effect of boundary layer height: in the winter, lower boundary height for mixing of NH_3 means more concentration. Deviations are also observed usually in spring, where it may be higher than in summer, during the period of manure/fertilizer

Preprints (www.preprints.org) | NOT PEER-REVIEWED | Posted: 21 August 2020 doi:10.20944/preprints202008.0468.v1

application. The dependence on emissions also extends to the type of source. When there is a constant source of emissions such as an industrial area, maximum [NH_3] may occur in winter due to the shallower atmospheric boundary layer. A key consideration to make is that the arithmetic seasonal mean may be affected greatly by outlier NH_3 emission events, deeming the geometric mean as more representative of background concentrations.

5.3. Long-term Trends

Although the effect of temperature and relative humidity is evident in the temporal trends discussed thus far, in the long-term, due to the expected smoothing out of meteorological factors, long-term trends in NH_3, if they exist, are mainly due to other factor(s). There have been observations of an increasing trend in NH_3 in the atmosphere in the recent years, despite almost constant or reducing emissions. It is likely that the changing chemical environment due to reducing acidic gases (SO_2 and NO_x) means that more NH_3 remains in the gas-phase with reduced available reducible species to form NH_4^+ in the particle phase.

There are numerous studies (see Table S1) indicating the long-term trends in [NH_3] over North America. The concentrations of NH_3 have been increasing across the US despite the nearly constant emission of NH_3. Butler *et al.* [53] using AMoN and Yao and Zhang [273] using NAPS, CAPMoN and AMoN network data provide evidence for this increase. Analysis of satellite (AIRS) derived NH_3 retrievals [97] shows that [NH_3] has increased by 0.056 ± 0.012 ppbv yr^{-1} (≈ 2.61 % yr^{-1}) over the US from 2002–2016. Ground-based measurements in Toronto, Canada show no significant increasing trend from 2003–2011 [274] and increasing ($\approx$20%) trend [273], however some sites in the United States show an increasing trend by up to 200%. Over the US, Yu *et al.* [122] examined long-term model simulated surface [NH_3], validated with network measurements. Their observation of increasing long-term trend of [NH_3] was demonstrated to be due to the decreasing emissions of SO_2 and NO_x contributing to roughly 2/3 and 1/3 of its increase over the US.

In China, the burgeoning population leads to increasing demand for animal and agricultural products. To meet this demand, there has been a sharp increase in the use of fertilizers for agriculture and concentrated animal feeding operations for producing livestock. This has led to the sharp increase of NH_3 emissions in China, especially in the North China Plain (NCP). A long-term record of [NH_3] is lacking for the nation. However, analysis of satellite (AIRS) derived long-term NH_3 retrievals [97] shows that NH_3 concentrations have increased over China by 0.076 ± 0.020 ppbv yr^{-1} (≈ 2.27 % yr^{-1}).

In the European Union, NH_3 emissions fell by 23% between 1990 and 2015 but increased between 2014 and 2015 by 1.8%, mainly because of increases in Germany, Spain, France, and the United Kingdom. In Germany, there has been a rising trend in NH_3 emissions, especially in the period from 2009. This is attributable mainly to inorganic nitrogen fertilizers. It must be noted that among the main pollutants in the EU, [NH_3] showed the least reduction (23%).

One of the longest and earliest long-term records of [NH_3] measurements, determined spectrophotometrically by Nesslerization, were available in Rijeka, Croatia from 1983. Alebic-Juretic [275] examined this record from 1983-2005 and the long-term trend of gas phase NH_3 showed a weak declining trend in two sites in the vicinity of the city over the period, despite estimated emissions reduction of $>$20%. Analysis of the 25-year long-term measured [NH_3] in Hungary by Horvath *et al.* [116] showed no decrease even in the period of large NH_3 emission reduction (from 1989), in fact, a small increase was observed. Over the United Kingdom, similar observations were made by Tang *et al.* [276] for the period from September 1996 to December 2005 despite a $\approx$12% reduction in emissions from 1990–2004. NH_3 emissions in Sweden decrease in the period (by 20.6% from 1993–2009), yet Ferm and Hellsten [277] observe an increase in [NH_3]. The strict control on NH_3 emissions in Netherlands saw a decrease in [NH_3] from 1993–2014, but there has been a subsequent increase despite emission reduction [163]. Analysis of satellite (AIRS) derived NH_3 retrievals [97] shows that NH_3 concentrations have increased over western Europe by 0.053 ± 0.021 ppbv yr^{-1} (≈ 1.83 % yr^{-1}).

Preprints (www.preprints.org) | NOT PEER-REVIEWED | Posted: 21 August 2020 doi:10.20944/preprints202008.0468.v1

Sutton *et al.* [278] posited interactions with SO_2, which has shown decreasing concentration, mask the expected decrease in [NH_3] due to slower rate of conversion from NH_3 to NH_4^+ and that reduced acidic species limit the potential for co-deposition and therefore reduce the dry deposition velocity, which leads to increased [NH_3]. This is the strongest reason explaining the various observed temporal variations of [NH_3]. Recent examination of [NH_3] measurements, remote sensing, and modeling data [88,97,121,122,148,163,246] provide evidence for this effect.

The temporal variation in [NH_3] is therefore highly dependent on the sources of emission and its temperature dependence. Warmer periods see elevated [NH_3]. Wetter periods see reduced [NH_3] due to lower temperatures and increased deposition. However, in the long-term, these meteorological effects are smoothed out. Additionally, due to generally reducing emissions, there should be a negative trend in [NH_3]. The studies above investigate the observed opposite trend of NH_3 concentration and emission and substantial evidence is presented for the significance of the changing chemical environment due to pollution control strategies.

6. Conclusions and Research Needs

This paper reviews around 540 publications in the quantification of atmospheric ammonia concentrations in the atmosphere through in situ measurements, satellite remote sensing inference, and model simulations. We summarize key points in line with the aims established at the beginning of this review:

NH_3 has been in the spotlight considering its increasing concentration despite reducing emissions over most regions of the globe. It is important to examine this chemical species due to its role in $PM_{2.5}$ formation, and mainly in the formation of NH_4NO_3. Its role in atmospheric new particle formation is of special interest as well. The main determinant of the concentration of ammonia in the atmosphere is its emissions. Due to the short lifetime of the gas-phase form, NH_3 is concentrated over regions of intensive agriculture and concentrated animal feeding operations such as the North China Plain, The Midwest US, the Indo-Gangetic plains, and pastoral lands of Europe. In some of these regions, [NH_3] can exceed 40 ppbv.

The variations in [NH_3] are expected to be temperature dependent: a virtue of the strong dependence on emission. Typically, at the diurnal scale, [NH_3] varies with the temperature, generally a function of insolation. There may be effects of vehicular emissions in pushing up [NH_3] and creating a bimodal daily cycle. However, many other factors such as transport, boundary layer height, deposition, fertilizer application time, traffic emissions and their interactions may result in unexpected variations of its atmospheric concentration. Seasonal and inter-annual variations are heavily meteorology dependent - warmer periods have higher [NH_3] and wetter/colder periods will have lesser [NH_3]. When examining long-term trends, which have been increasing over the last several years in most regions, there is mounting evidence for the importance of the chemical environment in determining the concentration of NH_3 in the atmosphere. In the long-term, the effect of meteorology is generally smoothed out and these long-term trends are mainly dictated by the chemical environment. Due to stringent regulations for the acid precursor gases (SO_2 and NO_x) in most parts of the world, as well as the comparatively constant NH_3 emissions, less NH_3 is taken up into the particle phase. Thus, the concentration of NH_3 is increased in the atmosphere. Sutton *et al.* [278] additionally suggests that dry deposition velocity is reduced due to reduced acidic precursor gases' concentration limiting the potential for co-deposition.

The quantification of [NH_3] through in situ observations, satellite remote sensing, and modeling comes with certain caveats. The main issue with in situ measurement of [NH_3] at the surface is the high cost for a comprehensive spatiotemporal coverage. [NH_3] is highly spatially variable, requiring any monitoring network to have a dense distribution of measurement stations. Online analyzers, while ideal, are not cost effective to implement. Further there may be non-linear negative bias in measured [NH_3] due to its stickiness (polar nature) to instrument surfaces. There is, therefore, a dearth of in situ measurements over remote areas on land, and especially over the oceans. Satellite-based

instruments are currently unable to resolve this gap due to the non-optimal thermal contrasts of the oceans for inference of ammonia mixing ratios from measure spectral radiances. Satellite remote sensing approaches need to be tuned specifically for the measurement of [NH_3]. Inference made from spectral radiances may be erroneous in circumstances such as night-time and times with cloudiness. The assumed fixed vertical NH_3 profile for the conversion of radiances to [NH_3] is problematic as well. There are other issues such as the fact that most remote sensing data is not from a geostationary constellation that provides continuous global coverage. Further, the spatial resolution is on the scale of several kilometers in diameter, a scale over which there can be significant variability in [NH_3]. Successful modeling is highly dependent on the accurate representation of the processes discussed in Section 3. Modeling of [NH_3] in the atmosphere over oceans is non-optimal due to negligible empirical datasets for validation, uncertain marine emissions, photolysis of dissolved organic nitrogen in the surface water or in the atmosphere [119], as well as different chemical environment (more acidic aerosols, more fine mode particles, sea salt alkalinity) affecting partitioning. Heretofore, the ammonia concentration over oceans (pptv levels) and remote areas (low ppbv levels) was considered insignificant. New research Yu *et al.* [5] suggests that nucleation is enhanced in the presence of pptv levels of atmospheric NH_3, making it important to understand ammonia over regions of its low concentration. Despite these issues, the three varied approaches compensate for each other's limitations to a fair degree and continue to keep improving. A synergistic approach of measurements↔satellite-inference↔modeling is the current research need, which will contribute towards improved understanding of ammonia in the atmosphere.

Supplementary Materials: The following are available online at http://www.mdpi.com/2073-4433/xx/1/5/s1, Table S1: In situ measurements of [NH_3], Table S2: Gas-Aerosol Equilibrium Models used in Chemical Transport Models.

Funding: This research was funded by NSF grant number AGS-1550816 and NASA grant number NNX17AG35G.

Conflicts of Interest: The authors declare no conflict of interest. The funders had no role in the design of the study; in the collection, analyses, or interpretation of data; in the writing of the manuscript, or in the decision to publish the results.

References

1. Sutton, M.A.; Erisman, J.W.; Dentener, F.; Möller, D. Ammonia in the environment: From ancient times to the present. *Environmental Pollution* **2008**, *156*, 583–604. doi:10.1016/j.envpol.2008.03.013.
2. Aneja, V.P.; Schlesinger, W.H.; Erisman, J.W. Effects of Agriculture upon the Air Quality and Climate: Research, Policy, and Regulations. *Environmental Science & Technology* **2009**, *43*, 4234–4240. doi:10.1021/es8024403.
3. Heald, C.L.; Geddes, J.A. The impact of historical land use change from 1850 to 2000 on secondary particulate matter and ozone. *Atmospheric Chemistry and Physics* **2016**, *16*, 14997–15010. doi:10.5194/acp-16-14997-2016.
4. Kirkby, J.; Curtius, J.; Almeida, J.; Dunne, E.; Duplissy, J.; Ehrhart, S.; Franchin, A.; Gagné, S.; Ickes, L.; Kürten, A.; Kupc, A.; Metzger, A.; Riccobono, F.; Rondo, L.; Schobesberger, S.; Tsagkogeorgas, G.; Wimmer, D.; Amorim, A.; Bianchi, F.; Breitenlechner, M.; David, A.; Dommen, J.; Downard, A.; Ehn, M.; Flagan, R.C.; Haider, S.; Hansel, A.; Hauser, D.; Jud, W.; Junninen, H.; Kreissl, F.; Kvashin, A.; Laaksonen, A.; Lehtipalo, K.; Lima, J.; Lovejoy, E.R.; Makhmutov, V.; Mathot, S.; Mikkilä, J.; Minginette, P.; Mogo, S.; Nieminen, T.; Onnela, A.; Pereira, P.; Petäjä, T.; Schnitzhofer, R.; Seinfeld, J.H.; Sipilä, M.; Stozhkov, Y.; Stratmann, F.; Tomé, A.; Vanhanen, J.; Viisanen, Y.; Vrtala, A.; Wagner, P.E.; Walther, H.; Weingartner, E.; Wex, H.; Winkler, P.M.; Carslaw, K.S.; Worsnop, D.R.; Baltensperger, U.; Kulmala, M. Role of sulphuric acid, ammonia and galactic cosmic rays in atmospheric aerosol nucleation. *Nature* **2011**, *476*, 429–433. doi:10.1038/nature10343.
5. Yu, F.; Nadykto, A.B.; Herb, J.; Luo, G.; Nazarenko, K.M.; Uvarova, L.A. H_2SO_4-H_2O-NH_3 ternary ion-mediated nucleation (TIMN): Kinetic-based model and comparison with CLOUD measurements. *Atmospheric Chemistry and Physics* **2018**, *18*, 17451–17474. doi:10.5194/acp-18-17451-2018.

6. Spengler, J.D.; Brauer, M.; Koutrakis, P. Acid air and health. *Environmental Science & Technology* **1990**, *24*, 946–956. doi:10.1021/es00077a002.
7. Mathur, R.; Dennis, R.L. Seasonal and annual modeling of reduced nitrogen compounds over the eastern United States: Emissions, ambient levels, and deposition amounts. *Journal of Geophysical Research: Atmospheres* **2003**, *108*. doi:10.1029/2002jd002794.
8. Galloway, J.N.; Dentener, F.J.; Capone, D.G.; Boyer, E.W.; Howarth, R.W.; Seitzinger, S.P.; Asner, G.P.; Cleveland, C.C.; Green, P.; Holland, E.A.; others. Nitrogen cycles: past, present, and future. *Biogeochemistry* **2004**, *70*, 153–226. doi:10.1007/s10533-004-0370-0.
9. Li, Y.; Schichtel, B.A.; Walker, J.T.; Schwede, D.B.; Chen, X.; Lehmann, C.M.B.; Puchalski, M.A.; Gay, D.A.; Collett, J.L. Increasing importance of deposition of reduced nitrogen in the United States. *Proceedings of the National Academy of Sciences* **2016**, *113*, 5874–5879. doi:10.1073/pnas.1525736113.
10. Kharol, S.K.; Shephard, M.W.; McLinden, C.A.; Zhang, L.; Sioris, C.E.; O'Brien, J.M.; Vet, R.; Cady-Pereira, K.E.; Hare, E.; Siemons, J.; Krotkov, N.A. Dry Deposition of Reactive Nitrogen From Satellite Observations of Ammonia and Nitrogen Dioxide Over North America. *Geophysical Research Letters* **2018**, *45*, 1157–1166. doi:10.1002/2017gl075832.
11. Bouwman, A.F.; Vuuren, D.P.V.; Derwent, R.G.; Posch, M. A global analysis of acidification and eutrophication of terrestrial ecosystems. *Water, Air, and Soil Pollution* **2002**, *141*, 349–382. doi:10.1023/a:1021398008726.
12. Fangmeier, A.; Hadwiger-Fangmeier, A.; der Eerden, L.V.; Jäger, H.J. Effects of atmospheric ammonia on vegetation— A review. *Environmental Pollution* **1994**, *86*, 43–82. doi:10.1016/0269-7491(94)90008-6.
13. Berman, T. Algal growth on organic compounds as nitrogen sources. *Journal of Plankton Research* **1999**, *21*, 1423–1437. doi:10.1093/plankt/21.8.1423.
14. Herndon, J.; Cochlan, W.P. Nitrogen utilization by the raphidophyte Heterosigma akashiwo: Growth and uptake kinetics in laboratory cultures. *Harmful Algae* **2007**, *6*, 260–270. doi:10.1016/j.hal.2006.08.006.
15. Paerl, H.W.; Scott, J.T. Throwing Fuel on the Fire: Synergistic Effects of Excessive Nitrogen Inputs and Global Warming on Harmful Algal Blooms. *Environmental Science & Technology* **2010**, *44*, 7756–7758. doi:10.1021/es102665e.
16. van Breemen, N.; Burrough, P.A.; Velthorst, E.J.; van Dobben, H.F.; de Wit, T.; Ridder, T.B.; Reijnders, H.F.R. Soil acidification from atmospheric ammonium sulphate in forest canopy throughfall. *Nature* **1982**, *299*, 548–550. doi:10.1038/299548a0.
17. Galloway, J.N. Acid deposition: Perspectives in time and space. *Water, Air, & Soil Pollution* **1995**, *85*, 15–24. doi:10.1007/bf00483685.
18. Bouwman, A.F.; Lee, D.S.; Asman, W.A.H.; Dentener, F.J.; Hoek, K.W.V.D.; Olivier, J.G.J. A global high-resolution emission inventory for ammonia. *Global Biogeochemical Cycles* **1997**, *11*, 561–587. doi:10.1029/97gb02266.
19. Paerl, H.W. Peer Reviewed: Connecting Atmospheric Nitrogen Deposition to Coastal Eutrophication. *Environmental Science & Technology* **2002**, *36*, 323A–326A. doi:10.1021/es022392a.
20. Ellis, R.A.; Jacob, D.J.; Sulprizio, M.P.; Zhang, L.; Holmes, C.D.; Schichtel, B.A.; Blett, T.; Porter, E.; Pardo, L.H.; Lynch, J.A. Present and future nitrogen deposition to national parks in the United States: critical load exceedances. *Atmospheric Chemistry and Physics* **2013**, *13*, 9083–9095. doi:10.5194/acp-13-9083-2013.
21. Payne, R.J.; Dise, N.B.; Stevens, C.J.; Gowing, D.J.; , Partners, B. Impact of nitrogen deposition at the species level. *Proceedings of the National Academy of Sciences* **2013**, *110*, 984–987. doi:10.1073/pnas.1214299109.
22. Cape, J.N.; van der Eerden, L.; Fangmeier, A.; Ayres, J.; Bareham, S.; Bobbink, R.; Branquinho, C.; Crittenden, P.; Cruz, C.; Dias, T.; Leith, I.; Martins-Loucao, M.A.; Pitcairn, C.; Sheppard, L.; Spranger, T.; Sutton, M.; van Dijk, N.; Wolseley, P. Critical Levels for Ammonia. In *Atmospheric Ammonia*; Springer Netherlands, 2009; pp. 375–382. doi:10.1007/978-1-4020-9121-6_22.
23. Krupa, S.V. Effects of atmospheric ammonia (NH3) on terrestrial vegetation: a review. *Environmental Pollution* **2003**, *124*, 179–221. doi:10.1016/s0269-7491(02)00434-7.
24. Kristensen, H.H.; Wathes, C.M. Ammonia and poultry welfare: a review. *World's Poultry Science Journal* **2000**, *56*, 235–245. doi:10.1079/wps20000018.
25. Wang, Y.M.; Meng, Q.P.; Guo, Y.M.; Wang, Y.Z.; Wang, Z.; Yao, Z.L.; Shan, T.Z. Effect of Atmospheric Ammonia on Growth Performance and Immunological Response of Broiler Chickens. *Journal of Animal and Veterinary Advances* **2010**, *9*, 2802–2806. doi:10.3923/javaa.2010.2802.2806.

26. Seedorf, J. BMTW - Wirkung von atmosphärischem Ammoniak auf Nutztiere eine Kurzübersicht. *Berl. Münch. Tierärztl. Wschr.* **2013**, *Berl. Münch. Tierärztl. Wschr.*, 96–103. doi:10.2376/0005-9366-126-96.
27. National Research Council. *Acute Exposure Guideline Levels for Selected Airborne Chemicals: Volume 6*; The National Academies Press: Washington, DC, 2008. doi:10.17226/12018.
28. Erisman, J.W.; Bleeker, A.; Galloway, J.; Sutton, M.S. Reduced nitrogen in ecology and the environment. *Environmental Pollution* **2007**, *150*, 140–149. doi:10.1016/j.envpol.2007.06.033.
29. Saxena, P.; Hudischewskyj, A.B.; Seigneur, C.; Seinfeld, J.H. A comparative study of equilibrium approaches to the chemical characterization of secondary aerosols. *Atmospheric Environment (1967)* **1986**, *20*, 1471–1483. doi:10.1016/0004-6981(86)90019-3.
30. Baek, B.H.; Aneja, V.P.; Tong, Q. Chemical coupling between ammonia, acid gases, and fine particles. *Environmental Pollution* **2004**, *129*, 89–98. doi:10.1016/j.envpol.2003.09.022.
31. Almeida, J.; Schobesberger, S.; Kürten, A.; Ortega, I.K.; Kupiainen-Määttä, O.; Praplan, A.P.; Adamov, A.; Amorim, A.; Bianchi, F.; Breitenlechner, M.; David, A.; Dommen, J.; Donahue, N.M.; Downard, A.; Dunne, E.; Duplissy, J.; Ehrhart, S.; Flagan, R.C.; Franchin, A.; Guida, R.; Hakala, J.; Hansel, A.; Heinritzi, M.; Henschel, H.; Jokinen, T.; Junninen, H.; Kajos, M.; Kangasluoma, J.; Keskinen, H.; Kupc, A.; Kurtén, T.; Kvashin, A.N.; Laaksonen, A.; Lehtipalo, K.; Leiminger, M.; Leppä, J.; Loukonen, V.; Makhmutov, V.; Mathot, S.; McGrath, M.J.; Nieminen, T.; Olenius, T.; Onnela, A.; Petäjä, T.; Riccobono, F.; Riipinen, I.; Rissanen, M.; Rondo, L.; Ruuskanen, T.; Santos, F.D.; Sarnela, N.; Schallhart, S.; Schnitzhofer, R.; Seinfeld, J.H.; Simon, M.; Sipilä, M.; Stozhkov, Y.; Stratmann, F.; Tomé, A.; Tröstl, J.; Tsagkogeorgas, G.; Vaattovaara, P.; Viisanen, Y.; Virtanen, A.; Vrtala, A.; Wagner, P.E.; Weingartner, E.; Wex, H.; Williamson, C.; Wimmer, D.; Ye, P.; Yli-Juuti, T.; Carslaw, K.S.; Kulmala, M.; Curtius, J.; Baltensperger, U.; Worsnop, D.R.; Vehkamäki, H.; Kirkby, J. Molecular understanding of sulphuric acid–amine particle nucleation in the atmosphere. *Nature* **2013**, *502*, 359–363. doi:10.1038/nature12663.
32. Racherla, P.N.; Adams, P.J. Sensitivity of global tropospheric ozone and fine particulate matter concentrations to climate change. *Journal of Geophysical Research* **2006**, *111*. doi:10.1029/2005jd006939.
33. Tsigaridis, K.; Krol, M.; Dentener, F.J.; Balkanski, Y.; Lathière, J.; Metzger, S.; Hauglustaine, D.A.; Kanakidou, M. Change in global aerosol composition since preindustrial times. *Atmospheric Chemistry and Physics* **2006**, *6*, 5143–5162. doi:10.5194/acp-6-5143-2006.
34. Schiferl, L.D.; Heald, C.L.; Nowak, J.B.; Holloway, J.S.; Neuman, J.A.; Bahreini, R.; Pollack, I.B.; Ryerson, T.B.; Wiedinmyer, C.; Murphy, J.G. An investigation of ammonia and inorganic particulate matter in California during the CalNex campaign. *Journal of Geophysical Research: Atmospheres* **2014**, *119*, 1883–1902. doi:10.1002/2013jd020765.
35. D'Hondt, P. Chemkar PM10: Chemische karakterisatie van fijn stof in Vlaanderen, 2006–2007. Technical Report D/2009/6871/015, Vlaamse Milieumaatschappij, 2009, [https://www.vmm.be/publicaties/chemkar-pm10-chemische-karakterisatie-van-fijn-stof-in-vlaanderen-2006-2007].
36. Dominici, F.; Wang, Y.; Correia, A.W.; Ezzati, M.; Pope, C.A.; Dockery, D.W. Chemical Composition of Fine Particulate Matter and Life Expectancy. *Epidemiology* **2015**, *26*, 556–564. doi:10.1097/ede.0000000000000297.
37. Döscher, A.; Gäggeler, H.W.; Schotterer, U.; Schwikowski, M. A historical record of ammonium concentrations from a glacier in the Alps. *Geophysical Research Letters* **1996**, *23*, 2741–2744. doi:10.1029/96gl02615.
38. Kang, S.; Mayewski, P.A.; Qin, D.; Yan, Y.; Zhang, D.; Hou, S.; Ren, J. Twentieth century increase of atmospheric ammonia recorded in Mount Everest ice core. *Journal of Geophysical Research: Atmospheres* **2002**, *107*, ACL13.1–9. doi:10.1029/2001jd001413.
39. Kellerhals, T.; Brütsch, S.; Sigl, M.; Knüsel, S.; Gäggeler, H.W.; Schwikowski, M. Ammonium concentration in ice cores: A new proxy for regional temperature reconstruction? *Journal of Geophysical Research* **2010**, *115*. doi:10.1029/2009jd012603.
40. Ball, S.; Hanson, D.; Eisele, F.; McMurry, P. Laboratory studies of particle nucleation: Initial results for H_2SO_4, H_2O and NH_3 vapors. *Journal of Geophysical Research: Atmospheres* **1999**, *104*, 23709–23718. doi:10.1029/1999JD900411.
41. Benson, D.R.; Erupe, M.E.; Lee, S.H. Laboratory-measured H_2SO_4-H_2O-NH_3 ternary homogeneous nucleation rates: Initial observations. *Geophysical Research Letters* **2009**, *36*, L15818. doi:10.1029/2009gl038728.

42. Yu, F. Effect of ammonia on new particle formation: A kinetic H_2SO_4-H_2O-NH_3 nucleation model constrained by laboratory measurements. *Journal of Geophysical Research: Atmospheres* **2006**, *111*. doi:10.1029/2005jd005968.
43. Wang, M.; Kong, W.; Marten, R.; He, X.C.; Chen, D.; Pfeifer, J.; Heitto, A.; Kontkanen, J.; Dada, L.; Kürten, A.; Yli-Juuti, T.; Manninen, H.E.; Amanatidis, S.; Amorim, A.; Baalbaki, R.; Baccarini, A.; Bell, D.M.; Bertozzi, B.; Bräkling, S.; Brilke, S.; Murillo, L.C.; Chiu, R.; Chu, B.; Menezes, L.P.D.; Duplissy, J.; Finkenzeller, H.; Carracedo, L.G.; Granzin, M.; Guida, R.; Hansel, A.; Hofbauer, V.; Krechmer, J.; Lehtipalo, K.; Lamkaddam, H.; Lampimäki, M.; Lee, C.P.; Makhmutov, V.; Marie, G.; Mathot, S.; Mauldin, R.L.; Mentler, B.; Müller, T.; Onnela, A.; Partoll, E.; Petäjä, T.; Philippov, M.; Pospisilova, V.; Ranjithkumar, A.; Rissanen, M.; Rörup, B.; Scholz, W.; Shen, J.; Simon, M.; Sipilä, M.; Steiner, G.; Stolzenburg, D.; Tham, Y.J.; Tomé, A.; Wagner, A.C.; Wang, D.S.; Wang, Y.; Weber, S.K.; Winkler, P.M.; Wlasits, P.J.; Wu, Y.; Xiao, M.; Ye, Q.; Zauner-Wieczorek, M.; Zhou, X.; Volkamer, R.; Riipinen, I.; Dommen, J.; Curtius, J.; Baltensperger, U.; Kulmala, M.; Worsnop, D.R.; Kirkby, J.; Seinfeld, J.H.; El-Haddad, I.; Flagan, R.C.; Donahue, N.M. Rapid growth of new atmospheric particles by nitric acid and ammonia condensation. *Nature* **2020**, *581*, 184–189. doi:10.1038/s41586-020-2270-4.
44. Boucher, O.; Randall, D.; Artaxo, P.; Bretherton, C.; Feingold, G.; Forster, P.; Kerminen, V.M.; Kondo, Y.; Liao, H.; Lohmann, U.; others. Clouds and Aerosols. In *Climate change 2013: the physical science basis. Contribution of Working Group I to the Fifth Assessment Report of the Intergovernmental Panel on Climate Change*; Cambridge University Press, 2013; pp. 571–657. doi:10.1017/cbo9781107415324.016.
45. Shindell, D.T.; Faluvegi, G.; Koch, D.M.; Schmidt, G.A.; Unger, N.; Bauer, S.E. Improved Attribution of Climate Forcing to Emissions. *Science* **2009**, *326*, 716–718. doi:10.1126/science.1174760.
46. Egner, H.; Eriksson, E. Current Data on the Chemical Composition of Air and Precipitation. *Tellus* **1955**, *7*, 266–271. doi:10.1111/j.2153-3490.1955.tb01161.x.
47. Junge, C.E. Recent Investigations in Air Chemistry. *Tellus* **1956**, *8*, 127–139. doi:10.3402/tellusa.v8i2.8971.
48. Appel, B.; Wall, S.; Tokiwa, Y.; Haik, M. Simultaneous nitric acid, particulate nitrate and acidity measurements in ambient air. *Atmospheric Environment (1967)* **1980**, *14*, 549–554. doi:10.1016/0004-6981(80)90084-0.
49. Pio, C.A.; Nunes, T.V.; Leal, R.M. Kinetic and thermodynamic behaviour of volatile ammonium compounds in industrial and marine atmospheres. *Atmospheric Environment. Part A. General Topics* **1992**, *26*, 505–512. doi:10.1016/0960-1686(92)90333-g.
50. Ferm, M. Method for determination of atmospheric ammonia. *Atmospheric Environment (1967)* **1979**, *13*, 1385–1393. doi:10.1016/0004-6981(79)90107-0.
51. Wyers, G.; Otjes, R.; Slanina, J. A continuous-flow denuder for the measurement of ambient concentrations and surface-exchange fluxes of ammonia. *Atmospheric Environment. Part A. General Topics* **1993**, *27*, 2085–2090. doi:10.1016/0960-1686(93)90280-c.
52. Puchalski, M.A.; Sather, M.E.; Walker, J.T.; Lehmann, C.M.B.; Gay, D.A.; Mathew, J.; Robarge, W.P. Passive ammonia monitoring in the United States: Comparing three different sampling devices. *Journal of Environmental Monitoring* **2011**, *13*, 3156. doi:10.1039/c1em10553a.
53. Butler, T.; Vermeylen, F.; Lehmann, C.; Likens, G.; Puchalski, M. Increasing ammonia concentration trends in large regions of the USA derived from the NADP/AMoN network. *Atmospheric Environment* **2016**, *146*, 132–140. Acid Rain and its Environmental Effects: Recent Scientific Advances, doi:10.1016/j.atmosenv.2016.06.033.
54. Sutton, M.A.; Tang, Y.S.; Miners, B.; Fowler, D. A New Diffusion Denuder System for Long-Term, Regional Monitoring of Atmospheric Ammonia and Ammonium. *Water, Air and Soil Pollution: Focus* **2001**, *1*, 145–156. doi:10.1023/a:1013138601753.
55. Tang, Y.S.; Cape, J.N.; Sutton, M.A. Development and Types of Passive Samplers for Monitoring Atmospheric NO2 and NH3 Concentrations. *The Scientific World JOURNAL* **2001**, *1*, 513–529. doi:10.1100/tsw.2001.82.
56. Berkhout, A.J.C.; Swart, D.P.J.; Volten, H.; Gast, L.F.L.; Haaima, M.; Verboom, H.; Stefess, G.; Hafkenscheid, T.; Hoogerbrugge, R. Replacing the AMOR with the miniDOAS in the ammonia monitoring network in the Netherlands. *Atmospheric Measurement Techniques* **2017**, *10*, 4099–4120. doi:10.5194/amt-10-4099-2017.

57. Lolkema, D.E.; Noordijk, H.; Stolk, A.P.; Hoogerbrugge, R.; van Zanten, M.C.; van Pul, W.A.J. The Measuring Ammonia in Nature (MAN) network in the Netherlands. *Biogeosciences* **2015**, *12*, 5133–5142. doi:10.5194/bg-12-5133-2015.
58. Fehsenfeld, F.C. Results from an informal intercomparison of ammonia measurement techniques. *Journal of Geophysical Research* **2002**, *107*. doi:10.1029/2001jd001327.
59. Nowak, J.B. Chemical ionization mass spectrometry technique for detection of dimethylsulfoxide and ammonia. *Journal of Geophysical Research* **2002**, *107*. doi:10.1029/2001jd001058.
60. Nowak, J.B.; Huey, L.G.; Russell, A.G.; Tian, D.; Neuman, J.A.; Orsini, D.; Sjostedt, S.J.; Sullivan, A.P.; Tanner, D.J.; Weber, R.J.; Nenes, A.; Edgerton, E.; Fehsenfeld, F.C. Analysis of urban gas phase ammonia measurements from the 2002 Atlanta Aerosol Nucleation and Real-Time Characterization Experiment (ANARChE). *Journal of Geophysical Research* **2006**, *111*. doi:10.1029/2006jd007113.
61. Nowak, J.B.; Neuman, J.A.; Kozai, K.; Huey, L.G.; Tanner, D.J.; Holloway, J.S.; Ryerson, T.B.; Frost, G.J.; McKeen, S.A.; Fehsenfeld, F.C. A chemical ionization mass spectrometry technique for airborne measurements of ammonia. *Journal of Geophysical Research: Atmospheres* **2007**, *112*. doi:10.1029/2006jd007589.
62. Norman, M.; Hansel, A.; Wisthaler, A. O2+ as reagent ion in the PTR-MS instrument: Detection of gas-phase ammonia. *International Journal of Mass Spectrometry* **2007**, *265*, 382–387. doi:10.1016/j.ijms.2007.06.010.
63. Norman, M.; Spirig, C.; Wolff, V.; Trebs, I.; Flechard, C.; Wisthaler, A.; Schnitzhofer, R.; Hansel, A.; Neftel, A. Intercomparison of ammonia measurement techniques at an intensively managed grassland site (Oensingen, Switzerland). *Atmospheric Chemistry and Physics* **2009**, *9*, 2635–2645. doi:10.5194/acp-9-2635-2009.
64. von Bobrutzki, K.; Braban, C.F.; Famulari, D.; Jones, S.K.; Blackall, T.; Smith, T.E.L.; Blom, M.; Coe, H.; Gallagher, M.; Ghalaieny, M.; McGillen, M.R.; Percival, C.J.; Whitehead, J.D.; Ellis, R.; Murphy, J.; Mohacsi, A.; Pogany, A.; Junninen, H.; Rantanen, S.; Sutton, M.A.; Nemitz, E. Field inter-comparison of eleven atmospheric ammonia measurement techniques. *Atmospheric Measurement Techniques* **2010**, *3*, 91–112. doi:10.5194/amt-3-91-2010.
65. Ellis, R.A.; Murphy, J.G.; Pattey, E.; van Haarlem, R.; O'Brien, J.M.; Herndon, S.C. Characterizing a Quantum Cascade Tunable Infrared Laser Differential Absorption Spectrometer (QC-TILDAS) for measurements of atmospheric ammonia. *Atmospheric Measurement Techniques* **2010**, *3*, 397–406. doi:10.5194/amt-3-397-2010.
66. Edner, H.; Amer, R.; Ragnarsson, P.; Rudin, M.; Svanberg, S. Atmospheric NH_3 monitoring by long-path UV absorption spectroscopy. Environment and Pollution Measurement Sensors and Systems; Nielsen, H.O., Ed. SPIE, 1990, pp. 14–20. doi:10.1117/12.20339.
67. Gall, R.; Perner, D.; Ladstätter-Weißenmayer, A. Simultaneous determination of NH3, SO2, NO and NO2 by direct UV-absorption in ambient air. *Fresenius' Journal of Analytical Chemistry* **1991**, *340*, 646–649. doi:10.1007/bf00321528.
68. Edner, H.; Ragnarson, P.; Spännare, S.; Svanberg, S. Differential optical absorption spectroscopy (DOAS) system for urban atmospheric pollution monitoring. *Applied Optics* **1993**, *32*, 327. doi:10.1364/ao.32.000327.
69. Mount, G.H.; Rumburg, B.; Havig, J.; Lamb, B.; Westberg, H.; Yonge, D.; Johnson, K.; Kincaid, R. Measurement of atmospheric ammonia at a dairy using differential optical absorption spectroscopy in the mid-ultraviolet. *Atmospheric Environment* **2002**, *36*, 1799–1810. doi:10.1016/s1352-2310(02)00158-9.
70. Neftel, A.; Blatter, A.; Staffelbach, T. Gas phase measurements of NH3and NH4 ± with Differential Optical Absorption Spectroscopy and Gas Stripping Scrubber in combination with Flow Injection Analysis. In *Physico-Chemical Behaviour of Atmospheric Pollutants*; Springer Netherlands, 1990; pp. 83–91. doi:10.1007/978-94-009-0567-2_13.
71. Mennen, M.; Elzakker, B.V.; Putten, E.V.; Uiterwijk, J.; Regts, T.; Hellemond, J.V.; Wyers, G.; Otjes, R.; Verhage, A.; Wouters, L.; Heffels, C.; Romer, F.; Beld, L.V.D.; Tetteroo, J. Evaluation of automatic ammonia monitors for application in an air quality monitoring network. *Atmospheric Environment* **1996**, *30*, 3239–3256. doi:10.1016/1352-2310(96)00079-9.
72. Volten, H.; Bergwerff, J.B.; Haaima, M.; Lolkema, D.E.; Berkhout, A.J.C.; van der Hoff, G.R.; Potma, C.J.M.; Kruit, R.J.W.; van Pul, W.A.J.; Swart, D.P.J. Two instruments based on differential optical absorption spectroscopy (DOAS) to measure accurate ammonia concentrations in the atmosphere. *Atmospheric Measurement Techniques* **2012**, *5*, 413–427. doi:10.5194/amt-5-413-2012.

73. Sintermann, J.; Dietrich, K.; Häni, C.; Bell, M.; Jocher, M.; Neftel, A. A miniDOAS instrument optimised for ammonia field measurements. *Atmospheric Measurement Techniques* **2016**, *9*, 2721–2734. doi:10.5194/amt-9-2721-2016.
74. ten Brink, H.; Otjes, R.; Jongejan, P.; Slanina, S. An instrument for semi-continuous monitoring of the size-distribution of nitrate, ammonium, sulphate and chloride in aerosol. *Atmospheric Environment* **2007**, *41*, 2768–2779. doi:10.1016/j.atmosenv.2006.11.041.
75. Rumsey, I.C.; Cowen, K.A.; Walker, J.T.; Kelly, T.J.; Hanft, E.A.; Mishoe, K.; Rogers, C.; Proost, R.; Beachley, G.M.; Lear, G.; Frelink, T.; Otjes, R.P. An assessment of the performance of the Monitor for AeRosols and GAses in ambient air (MARGA): a semi-continuous method for soluble compounds. *Atmospheric Chemistry and Physics* **2014**, *14*, 5639–5658. doi:10.5194/acp-14-5639-2014.
76. Schwab, J.J.; Li, Y.; Bae, M.S.; Demerjian, K.L.; Hou, J.; Zhou, X.; Jensen, B.; Pryor, S.C. A Laboratory Intercomparison of Real-Time Gaseous Ammonia Measurement Methods. *Environmental Science & Technology* **2007**, *41*, 8412–8419. doi:10.1021/es070354r.
77. Erisman, J. Instrument development and application in studies and monitoring of ambient ammonia. *Atmospheric Environment* **2001**, *35*, 1913–1922. doi:10.1016/s1352-2310(00)00544-6.
78. Harrison, R.M.; Allen, A. Measurements of atmospheric HNO3, HCl and associated species on a small network in eastern England. *Atmospheric Environment. Part A. General Topics* **1990**, *24*, 369–376. doi:10.1016/0960-1686(90)90116-5.
79. Beer, R.; Shephard, M.W.; Kulawik, S.S.; Clough, S.A.; Eldering, A.; Bowman, K.W.; Sander, S.P.; Fisher, B.M.; Payne, V.H.; Luo, M.; Osterman, G.B.; Worden, J.R. First satellite observations of lower tropospheric ammonia and methanol. *Geophysical Research Letters* **2008**, *35*. doi:10.1029/2008gl033642.
80. Clarisse, L.; Clerbaux, C.; Dentener, F.; Hurtmans, D.; Coheur, P.F. Global ammonia distribution derived from infrared satellite observations. *Nature Geoscience* **2009**, *2*, 479–483. doi:10.1038/ngeo551.
81. Coheur, P.F.; Clarisse, L.; Turquety, S.; Hurtmans, D.; Clerbaux, C. IASI measurements of reactive trace species in biomass burning plumes. *Atmospheric Chemistry and Physics* **2009**, *9*, 5655–5667. doi:10.5194/acp-9-5655-2009.
82. Clerbaux, C.; Boynard, A.; Clarisse, L.; George, M.; Hadji-Lazaro, J.; Herbin, H.; Hurtmans, D.; Pommier, M.; Razavi, A.; Turquety, S.; Wespes, C.; Coheur, P.F. Monitoring of atmospheric composition using the thermal infrared IASI/MetOp sounder. *Atmospheric Chemistry and Physics* **2009**, *9*, 6041–6054. doi:10.5194/acp-9-6041-2009.
83. Clarisse, L.; Shephard, M.W.; Dentener, F.; Hurtmans, D.; Cady-Pereira, K.; Karagulian, F.; Damme, M.V.; Clerbaux, C.; Coheur, P.F. Satellite monitoring of ammonia: A case study of the San Joaquin Valley. *Journal of Geophysical Research* **2010**, *115*. doi:10.1029/2009jd013291.
84. Pinder, R.W.; Walker, J.T.; Bash, J.O.; Cady-Pereira, K.E.; Henze, D.K.; Luo, M.; Osterman, G.B.; Shephard, M.W. Quantifying spatial and seasonal variability in atmospheric ammonia with in situ and space-based observations. *Geophysical Research Letters* **2011**, *38*, L04802. doi:10.1029/2010gl046146.
85. Ginoux, P.; Clarisse, L.; Clerbaux, C.; Coheur, P.F.; Dubovik, O.; Hsu, N.C.; Damme, M.V. Mixing of dust and NH_3 observed globally over anthropogenic dust sources. *Atmospheric Chemistry and Physics* **2012**, *12*, 7351–7363. doi:10.5194/acp-12-7351-2012.
86. R'Honi, Y.; Clarisse, L.; Clerbaux, C.; Hurtmans, D.; Duflot, V.; Turquety, S.; Ngadi, Y.; Coheur, P.F. Exceptional emissions of NH_3 and HCOOH in the 2010 Russian wildfires. *Atmospheric Chemistry and Physics* **2013**, *13*, 4171–4181. doi:10.5194/acp-13-4171-2013.
87. Zhu, L.; Henze, D.K.; Cady-Pereira, K.E.; Shephard, M.W.; Luo, M.; Pinder, R.W.; Bash, J.O.; Jeong, G.R. Constraining U.S. ammonia emissions using TES remote sensing observations and the GEOS-Chem adjoint model. *Journal of Geophysical Research: Atmospheres* **2013**, *118*, 3355–3368. doi:10.1002/jgrd.50166.
88. van Damme, M.; Wichink Kruit, R.J.; Schaap, M.; Clarisse, L.; Clerbaux, C.; Coheur, P.F.; Dammers, E.; Dolman, A.J.; Erisman, J.W. Evaluating 4 years of atmospheric ammonia (NH_3) over Europe using IASI satellite observations and LOTOS-EUROS model results. *Journal of Geophysical Research: Atmospheres* **2014**, *119*, 9549–9566. doi:10.1002/2014JD021911.
89. Sun, K.; Cady-Pereira, K.; Miller, D.J.; Tao, L.; Zondlo, M.A.; Nowak, J.B.; Neuman, J.A.; Mikoviny, T.; Müller, M.; Wisthaler, A.; Scarino, A.J.; Hostetler, C.A. Validation of TES ammonia observations at the single pixel scale in the San Joaquin Valley during DISCOVER-AQ. *Journal of Geophysical Research: Atmospheres* **2015**, *120*, 5140–5154. doi:10.1002/2014jd022846.

90. Luo, M.; Shephard, M.W.; Cady-Pereira, K.E.; Henze, D.K.; Zhu, L.; Bash, J.O.; Pinder, R.W.; Capps, S.L.; Walker, J.T.; Jones, M.R. Satellite observations of tropospheric ammonia and carbon monoxide: Global distributions, regional correlations and comparisons to model simulations. *Atmospheric Environment* **2015**, *106*, 262–277. doi:10.1016/j.atmosenv.2015.02.007.
91. Shephard, M.W.; McLinden, C.A.; Cady-Pereira, K.E.; Luo, M.; Moussa, S.G.; Leithead, A.; Liggio, J.; Staebler, R.M.; Akingunola, A.; Makar, P.; Lehr, P.; Zhang, J.; Henze, D.K.; Millet, D.B.; Bash, J.O.; Zhu, L.; Wells, K.C.; Capps, S.L.; Chaliyakunnel, S.; Gordon, M.; Hayden, K.; Brook, J.R.; Wolde, M.; Li, S.M. Tropospheric Emission Spectrometer (TES) satellite observations of ammonia, methanol, formic acid, and carbon monoxide over the Canadian oil sands: validation and model evaluation. *Atmospheric Measurement Techniques* **2015**, *8*, 5189–5211. doi:10.5194/amt-8-5189-2015.
92. Shephard, M.W.; Cady-Pereira, K.E. Cross-track Infrared Sounder (CrIS) satellite observations of tropospheric ammonia. *Atmospheric Measurement Techniques* **2015**, *8*, 1323–1336. doi:10.5194/amt-8-1323-2015.
93. Damme, M.V.; Erisman, J.W.; Clarisse, L.; Dammers, E.; Whitburn, S.; Clerbaux, C.; Dolman, A.J.; Coheur, P.F. Worldwide spatiotemporal atmospheric ammonia (NH_3) columns variability revealed by satellite. *Geophysical Research Letters* **2015**, *42*, 8660–8668. doi:10.1002/2015gl065496.
94. Dammers, E.; Palm, M.; Van Damme, M.; Vigouroux, C.; Smale, D.; Conway, S.; Toon, G.C.; Jones, N.; Nussbaumer, E.; Warneke, T.; Petri, C.; Clarisse, L.; Clerbaux, C.; Hermans, C.; Lutsch, E.; Strong, K.; Hannigan, J.W.; Nakajima, H.; Morino, I.; Herrera, B.; Stremme, W.; Grutter, M.; Schaap, M.; Wichink Kruit, R.J.; Notholt, J.; Coheur, P.F.; Erisman, J.W. An evaluation of IASI-NH_3 with ground-based Fourier transform infrared spectroscopy measurements. *Atmospheric Chemistry and Physics* **2016**, *16*, 10351–10368. doi:10.5194/acp-16-10351-2016.
95. Höpfner, M.; Volkamer, R.; Grabowski, U.; Grutter, M.; Orphal, J.; Stiller, G.; von Clarmann, T.; Wetzel, G. First detection of ammonia (NH_3) in the Asian summer monsoon upper troposphere. *Atmospheric Chemistry and Physics* **2016**, *16*, 14357–14369. doi:10.5194/acp-16-14357-2016.
96. Warner, J.X.; Wei, Z.; Strow, L.L.; Dickerson, R.R.; Nowak, J.B. The global tropospheric ammonia distribution as seen in the 13-year AIRS measurement record. *Atmospheric Chemistry and Physics* **2016**, *16*, 5467–5479. doi:10.5194/acp-16-5467-2016.
97. Warner, J.X.; Dickerson, R.R.; Wei, Z.; Strow, L.L.; Wang, Y.; Liang, Q. Increased atmospheric ammonia over the world's major agricultural areas detected from space. *Geophysical Research Letters* **2017**, *44*, 2875–2884. doi:10.1002/2016GL072305.
98. Bray, C.D.; Battye, W.; Aneja, V.P.; Tong, D.; Lee, P.; Tang, Y.; Nowak, J.B. Evaluating ammonia (NH 3) predictions in the NOAA National Air Quality Forecast Capability (NAQFC) using in-situ aircraft and satellite measurements from the CalNex2010 campaign. *Atmospheric Environment* **2017**, *163*, 65–76. doi:10.1016/j.atmosenv.2017.05.032.
99. Hickman, J.E.; Dammers, E.; Galy-Lacaux, C.; van der Werf, G.R. Satellite evidence of substantial rain-induced soil emissions of ammonia across the Sahel. *Atmospheric Chemistry and Physics* **2018**, *18*, 16713–16727. doi:10.5194/acp-18-16713-2018.
100. Damme, M.V.; Clarisse, L.; Whitburn, S.; Hadji-Lazaro, J.; Hurtmans, D.; Clerbaux, C.; Coheur, P.F. Industrial and agricultural ammonia point sources exposed. *Nature* **2018**, *564*, 99–103. doi:10.1038/s41586-018-0747-1.
101. Adams, C.; McLinden, C.A.; Shephard, M.W.; Dickson, N.; Dammers, E.; Chen, J.; Makar, P.; Cady-Pereira, K.E.; Tam, N.; Kharol, S.K.; Lamsal, L.N.; Krotkov, N.A. Satellite-derived emissions of carbon monoxide, ammonia, and nitrogen dioxide from the 2016 Horse River wildfire in the Fort McMurray area. *Atmospheric Chemistry and Physics* **2019**, *19*, 2577–2599. doi:10.5194/acp-19-2577-2019.
102. Clarisse, L.; Damme, M.V.; Gardner, W.; Coheur, P.F.; Clerbaux, C.; Whitburn, S.; Hadji-Lazaro, J.; Hurtmans, D. Atmospheric ammonia (NH3) emanations from Lake Natron's saline mudflats. *Scientific Reports* **2019**, *9*. doi:10.1038/s41598-019-39935-3.
103. Clarisse, L.; Van Damme, M.; Clerbaux, C.; Coheur, P.F. Tracking down global NH_3 point sources with wind-adjusted superresolution. *Atmospheric Measurement Techniques* **2019**, *12*, 5457–5473. doi:10.5194/amt-12-5457-2019.
104. Shephard, M.W.; Dammers, E.; Cady-Pereira, K.E.; Kharol, S.K.; Thompson, J.; Gainariu-Matz, Y.; Zhang, J.; McLinden, C.A.; Kovachik, A.; Moran, M.; Bittman, S.; Sioris, C.E.; Griffin, D.; Alvarado, M.J.;

Lonsdale, C.; Savic-Jovcic, V.; Zheng, Q. Ammonia measurements from space with the Cross-track Infrared Sounder: characteristics and applications. *Atmospheric Chemistry and Physics* **2020**, *20*, 2277–2302. doi:10.5194/acp-20-2277-2020.

105. Someya, Y.; Imasu, R.; Shiomi, K.; Saitoh, N. Atmospheric ammonia retrieval from the TANSO-FTS/GOSAT thermal infrared sounder. *Atmospheric Measurement Techniques* **2020**, *13*, 309–321. doi:10.5194/amt-13-309-2020.
106. Simmons, J.W.; Gordy, W. Structure of the Inversion Spectrum of Ammonia. *Physical Review* **1948**, *73*, 713–718. doi:10.1103/PhysRev.73.713.
107. Rodgers, C.D.; Connor, B.J. Intercomparison of remote sounding instruments. *Journal of Geophysical Research: Atmospheres* **2003**, *108*, n/a–n/a. doi:10.1029/2002jd002299.
108. Heald, C.L.; Jr., J.L.C.; Lee, T.; Benedict, K.B.; Schwandner, F.M.; Li, Y.; Clarisse, L.; Hurtmans, D.R.; Damme, M.V.; Clerbaux, C.; Coheur, P.F.; Philip, S.; Martin, R.V.; Pye, H.O.T. Atmospheric ammonia and particulate inorganic nitrogen over the United States. *Atmospheric Chemistry and Physics* **2012**, *12*, 10295–10312. doi:10.5194/acp-12-10295-2012.
109. De Meij, A.; Thunis, P.; Bessagnet, B.; Cuvelier, C. The sensitivity of the CHIMERE model to emissions reduction scenarios on air quality in Northern Italy. *Atmospheric environment* **2009**, *43*, 1897–1907. doi:10.1016/j.atmosenv.2008.12.036.
110. Gilliland, A.B.; Dennis, R.L.; Roselle, S.J.; Pierce, T.E. Seasonal NH_3 emission estimates for the eastern United States based on ammonium wet concentrations and an inverse modeling method. *Journal of Geophysical Research: Atmospheres* **2003**, *108*. doi:10.1029/2002jd003063.
111. Gilliland, A.B.; Appel, K.W.; Pinder, R.W.; Dennis, R.L. Seasonal NH_3 emissions for the continental united states: Inverse model estimation and evaluation. *Atmospheric Environment* **2006**, *40*, 4986–4998. doi:10.1016/j.atmosenv.2005.12.066.
112. Frohn, L. A study of long-term high-resolution air pollution modelling. PhD thesis, Aarhus Universtet, 2004.
113. Brandt, J.; Silver, J.D.; Frohn, L.; Geels, C.; Gross, A.; Hansen, A.B.; Hansen, K.M.; Hedegaard, G.B.; Skjøth, C.A.; Villadsen, H.; others. An integrated model study for Europe and North America using the Danish Eulerian Hemispheric Model with focus on intercontinental transport of air pollution. *Atmospheric Environment* **2012**, *53*, 156–176. doi:10.1016/j.atmosenv.2012.01.011.
114. Geels, C.; Andersen, H.V.; Skjøth, C.A.; Christensen, J.H.; Ellermann, T.; Løfstrøm, P.; Gyldenkærne, S.; Brandt, J.; Hansen, K.M.; Frohn, L.M.; Hertel, O. Improved modelling of atmospheric ammonia over Denmark using the coupled modelling system DAMOS. *Biogeosciences* **2012**, *9*, 2625–2647. doi:10.5194/bg-9-2625-2012.
115. Fagerli, H.; Aas, W. Trends of nitrogen in air and precipitation: Model results and observations at EMEP sites in Europe, 1980–2003. *Environmental Pollution* **2008**, *154*, 448–461. doi:10.1016/j.envpol.2008.01.024.
116. Horvath, L.; Fagerli, H.; Sutton, M.A. Long-Term Record (1981–2005) of Ammonia and Ammonium Concentrations at K-Puszta Hungary and the Effect of Sulphur Dioxide Emission Change on Measured and Modelled Concentrations. In *Atmospheric Ammonia*; Springer, 2009; pp. 181–185. doi:10.1007/978-1-4020-9121-6_12.
117. Walker, J.M.; Philip, S.; Martin, R.V.; Seinfeld, J.H. Simulation of nitrate, sulfate, and ammonium aerosols over the United States. *Atmospheric Chemistry and Physics* **2012**, *12*, 11213–11227. doi:10.5194/acp-12-11213-2012.
118. Zhang, L.; Jacob, D.J.; Knipping, E.M.; Kumar, N.; Munger, J.W.; Carouge, C.C.; van Donkelaar, A.; Wang, Y.X.; Chen, D. Nitrogen deposition to the United States: distribution, sources, and processes. *Atmospheric Chemistry and Physics* **2012**, *12*, 4539–4554. doi:10.5194/acp-12-4539-2012.
119. Paulot, F.; Jacob, D.J.; Johnson, M.T.; Bell, T.G.; Baker, A.R.; Keene, W.C.; Lima, I.D.; Doney, S.C.; Stock, C.A. Global oceanic emission of ammonia: Constraints from seawater and atmospheric observations. *Global Biogeochemical Cycles* **2015**, *29*, 1165–1178. doi:10.1002/2015gb005106.
120. Zhu, L.; Henze, D.; Bash, J.; Jeong, G.R.; Cady-Pereira, K.; Shephard, M.; Luo, M.; Paulot, F.; Capps, S. Global evaluation of ammonia bidirectional exchange and livestock diurnal variation schemes. *Atmospheric Chemistry and Physics* **2015**, *15*, 12823–12843. doi:10.5194/acp-15-12823-2015.
121. Schiferl, L.D.; Heald, C.L.; Damme, M.V.; Clarisse, L.; Clerbaux, C.; Coheur, P.F.; Nowak, J.B.; Neuman, J.A.; Herndon, S.C.; Roscioli, J.R.; Eilerman, S.J. Interannual variability of ammonia concentrations over

the United States: sources and implications. *Atmospheric Chemistry and Physics* **2016**, *16*, 12305–12328. doi:10.5194/acp-16-12305-2016.

122. Yu, F.; Nair, A.A.; Luo, G. Long-term trend of gaseous ammonia over the United States: Modeling and comparison with observations. *Journal of Geophysical Research: Atmospheres* **2018**, *0*. doi:10.1029/2018JD028412.
123. Nair, A.A.; Yu, F.; Luo, G. Spatioseasonal Variations of Atmospheric Ammonia Concentrations Over the United States: Comprehensive Model-Observation Comparison. *Journal of Geophysical Research: Atmospheres* **2019**, *124*, 6571–6582. doi:10.1029/2018JD030057.
124. Paulot, F.; Jacob, D.J.; Pinder, R.W.; Bash, J.O.; Travis, K.; Henze, D.K. Ammonia emissions in the United States, European Union, and China derived by high-resolution inversion of ammonium wet deposition data: Interpretation with a new agricultural emissions inventory (MASAGE_NH_3). *Journal of Geophysical Research: Atmospheres* **2014**, *119*, 4343–4364. doi:10.1002/2013jd021130.
125. van Damme, M.; Clarisse, L.; Heald, C.L.; Hurtmans, D.; Ngadi, Y.; Clerbaux, C.; Dolman, A.J.; Erisman, J.W.; Coheur, P.F. Global distributions, time series and error characterization of atmospheric ammonia (NH_3) from IASI satellite observations. *Atmospheric Chemistry and Physics* **2014**, *14*, 2905–2922. doi:10.5194/acp-14-2905-2014.
126. Langner, J.; Andersson, C.; Engardt, M. Atmospheric input of nitrogen to the Baltic Sea basin: present situation, variability due to meteorology and impact of climate change. *Boreal Environment Research* **2009**, *14*, 226–237.
127. Pinder, R.W.; Adams, P.J.; Pandis, S.N.; Gilliland, A.B. Temporally resolved ammonia emission inventories: Current estimates, evaluation tools, and measurement needs. *Journal of Geophysical Research* **2006**, *111*. doi:10.1029/2005jd006603.
128. Murphy, B.N.; Pandis, S.N. Simulating the Formation of Semivolatile Primary and Secondary Organic Aerosol in a Regional Chemical Transport Model. *Environmental Science & Technology* **2009**, *43*, 4722–4728. doi:10.1021/es803168a.
129. Tsimpidi, A.P.; Karydis, V.A.; Zavala, M.; Lei, W.; Molina, L.; Ulbrich, I.M.; Jimenez, J.L.; Pandis, S.N. Evaluation of the volatility basis-set approach for the simulation of organic aerosol formation in the Mexico City metropolitan area. *Atmospheric Chemistry and Physics* **2010**, *10*, 525–546. doi:10.5194/acp-10-525-2010.
130. Karydis, V.A.; Tsimpidi, A.P.; Fountoukis, C.; Nenes, A.; Zavala, M.; Lei, W.; Molina, L.T.; Pandis, S.N. Simulating the fine and coarse inorganic particulate matter concentrations in a polluted megacity. *Atmospheric Environment* **2010**, *44*, 608–620. doi:10.1016/j.atmosenv.2009.11.023.
131. Fountoukis, C.; Racherla, P.N.; van der Gon, H.A.C.D.; Polymeneas, P.; Charalampidis, P.E.; Pilinis, C.; Wiedensohler, A.; Dall'Osto, M.; O'Dowd, C.; Pandis, S.N. Evaluation of a three-dimensional chemical transport model (PMCAMx) in the European domain during the EUCAARI May 2008 campaign. *Atmospheric Chemistry and Physics* **2011**, *11*, 10331–10347. doi:10.5194/acp-11-10331-2011.
132. de Meij, A.; Krol, M.; Dentener, F.; Vignati, E.; Cuvelier, C.; Thunis, P. The sensitivity of aerosol in Europe to two different emission inventories and temporal distribution of emissions. *Atmospheric Chemistry and Physics* **2006**, *6*, 4287–4309. doi:10.5194/acp-6-4287-2006.
133. Hertel, O.; Christensen, J.; Runge, E.H.; Asman, W.A.; Berkowicz, R.; Hovmand, M.F.; Øystein Hov. Development and testing of a new variable scale air pollution model— ACDEP. *Atmospheric Environment* **1995**, *29*, 1267–1290. doi:10.1016/1352-2310(95)00067-9.
134. Hertel, O.; Ambelas Skjøth, C.; Brandt, J.; Christensen, J.H.; Frohn, L.M.; Frydendall, J. Operational mapping of atmospheric nitrogen deposition to the Baltic Sea. *Atmospheric Chemistry and Physics* **2003**, *3*, 2083–2099. doi:10.5194/acp-3-2083-2003.
135. Gyldenkaerne, S.; Ambelas Skjøth, C.; Hertel, O.; Ellermann, T. A dynamical ammonia emission parameterization for use in air pollution models. *Journal of Geophysical Research: Atmospheres* **2005**, *110*. doi:10.1029/2004JD005459.
136. de Leeuw, G.; Spokes, L.; Jickells, T.; Skjøth, C.A.; Hertel, O.; Vignati, E.; Tamm, S.; Schulz, M.; Sørensen, L.L.; Pedersen, B.; Klein, L.; Schlünzen, K. Atmospheric nitrogen inputs into the North Sea: effect on productivity. *Continental Shelf Research* **2003**, *23*, 1743–1755. European Land-Ocean Interaction, doi:10.1016/j.csr.2003.06.011.

137. Skjøth, C.A.; Hertel, O.; Ellermann, T. Use of the ACDEP trajectory model in the Danish nation-wide Background Monitoring Programme. *Physics and Chemistry of the Earth, Parts A/B/C* **2002**, *27*, 1469–1477. doi:10.1016/S1474-7065(02)00149-3.
138. Skjøth, C.A.; Hertel, O.; Gyldenkaerne, S.; Ellermann, T. Implementing a dynamical ammonia emission parameterization in the large-scale air pollution model ACDEP. *Journal of Geophysical Research: Atmospheres* **2004**, *109*. doi:10.1029/2003JD003895.
139. Skjøth, C.A.; Geels, C.; Berge, H.; Gyldenkærne, S.; Fagerli, H.; Ellermann, T.; Frohn, L.M.; Christensen, J.; Hansen, K.M.; Hansen, K.; Hertel, O. Spatial and temporal variations in ammonia emissions—a freely accessible model code for Europe. *Atmospheric Chemistry and Physics* **2011**, *11*, 5221–5236. doi:10.5194/acp-11-5221-2011.
140. Makar, P.; Bouchet, V.; Nenes, A. Inorganic chemistry calculations using HETV– a vectorized solver for the SO42–NO3–NH4+ system based on the ISORROPIA algorithms. *Atmospheric Environment* **2003**, *37*, 2279–2294. doi:10.1016/S1352-2310(03)00074-8.
141. Makar, P.A.; Moran, M.D.; Zheng, Q.; Cousineau, S.; Sassi, M.; Duhamel, A.; Besner, M.; Davignon, D.; Crevier, L.P.; Bouchet, V.S. Modelling the impacts of ammonia emissions reductions on North American air quality. *Atmospheric Chemistry and Physics* **2009**, *9*, 7183–7212. doi:10.5194/acp-9-7183-2009.
142. Barrett, K.; Seland, Ø.; Foss, A.; Mylona, S.; Sandnes, H.; Styve, H.; Tarrason, L. European Transboundary Acidifying Air Pollution: Ten years calculated fields and budgets to the end of the first Sulphur protocol. Technical report, Norske Meteorologiske Inst., Oslo (Norway), 1995.
143. Fournier, N.; Pais, V.; Sutton, M.; Weston, K.; Dragosits, U.; Tang, S.; Aherne, J. Parallelisation and application of a multi-layer atmospheric transport model to quantify dispersion and deposition of ammonia over the British Isles. *Environmental Pollution* **2002**, *116*, 95–107. doi:10.1016/S0269-7491(01)00146-4.
144. Fournier, N.; Tang, Y.S.; Dragosits, U.; Kluizenaar, Y.D.; Sutton, M.A. Regional Atmospheric Budgets of Reduced Nitrogen Over the British Isles Assessed Using a Multi-Layer Atmospheric Transport Model. *Water, Air, and Soil Pollution* **2005**, *162*, 331–351. doi:10.1007/s11270-005-7249-0.
145. Fournier, N.; Weston, K.J.; Dore, A.J.; Sutton, M.A. Modelling the wet deposition of reduced nitrogen over the British Isles using a Lagrangian multi-layer atmospheric transport model. *Quarterly Journal of the Royal Meteorological Society* **2005**, *131*, 703–722. doi:10.1256/qj.04.76.
146. Dore, A.; Vieno, M.; Tang, Y.; Dragosits, U.; Dosio, A.; Weston, K.; Sutton, M. Modelling the atmospheric transport and deposition of sulphur and nitrogen over the United Kingdom and assessment of the influence of SO2 emissions from international shipping. *Atmospheric Environment* **2007**, *41*, 2355–2367. doi:10.1016/j.atmosenv.2006.11.013.
147. Sutton, M.; Dragosits, U.; Simmons, I.; Tang, Y.; Hellsten, S.; Love, L.; Vieno, M.; Skiba, U.; di Marco, C.; Storeton-West, R.; Fowler, D.; Williams, J.; North, P.; Hobbs, P.; Misselbrook, T. Monitoring and modelling trace-gas changes following the 2001 outbreak of Foot and Mouth Disease to reduce the uncertainties in agricultural emissions abatement. *Environmental Science & Policy* **2006**, *9*, 407–422. doi:10.1016/j.envsci.2006.04.001.
148. Tang, Y.S.; Braban, C.F.; Dragosits, U.; Dore, A.J.; Simmons, I.; van Dijk, N.; Poskitt, J.; Pereira, G.D.S.; Keenan, P.O.; Conolly, C.; Vincent, K.; Smith, R.I.; Heal, M.R.; Sutton, M.A. Drivers for spatial, temporal and long-term trends in atmospheric ammonia and ammonium in the UK. *Atmospheric Chemistry and Physics* **2018**, *18*, 705–733. doi:10.5194/acp-18-705-2018.
149. Vieno, M. Use of an atmospheric chemistry-transport model (FRAME) over the UK and the development of its numerical and physical schemes. PhD thesis, University of Edinburgh, 2005.
150. Sutton, M.A.; Tang, Y.S.; Dragosits, U.; Fournier, N.; Dore, A.J.; Smith, R.I.; Weston, K.J.; Fowler, D. A Spatial Analysis of Atmospheric Ammonia and Ammonium in the U.K. *The Scientific World JOURNAL* **2001**, *1*, 275–286. doi:10.1100/tsw.2001.313.
151. Sutton, M.; Milford, C.; Dragosits, U.; Place, C.; Singles, R.; Smith, R.; Pitcairn, C.; Fowler, D.; Hill, J.; ApSimon, H.; Ross, C.; Hill, R.; Jarvis, S.; Pain, B.; Phillips, V.; Harrison, R.; Moss, D.; Webb, J.; Espenhahn, S.; Lee, D.; Hornung, M.; Ullyett, J.; Bull, K.; Emmett, B.; Lowe, J.; Wyers, G. Dispersion, deposition and impacts of atmospheric ammonia: quantifying local budgets and spatial variability. *Environmental Pollution* **1998**, *102*, 349–361. Nitrogen, the Confer-N-s First International Nitrogen Conference 1998, doi:10.1016/S0269-7491(98)80054-7.

152. Hellsten, S.; Dragosits, U.; Place, C.; Vieno, M.; Dore, A.; Misselbrook, T.; Tang, Y.; Sutton, M. Modelling the spatial distribution of ammonia emissions in the UK. *Environmental Pollution* **2008**, *154*, 370–379. Reduced Nitrogen in Ecology and the Environment, doi:10.1016/j.envpol.2008.02.017.
153. Singles, R.; Sutton, M.; Weston, K. A multi-layer model to describe the atmospheric transport and deposition of ammonia in Great Britain. *Atmospheric Environment* **1998**, *32*, 393–399. doi:10.1016/S1352-2310(97)83467-X.
154. Hallsworth, S.; Dore, A.; Bealey, W.; Dragosits, U.; Vieno, M.; Hellsten, S.; Tang, Y.; Sutton, M. The role of indicator choice in quantifying the threat of atmospheric ammonia to the 'Natura 2000' network. *Environmental Science & Policy* **2010**, *13*, 671–687. doi:10.1016/j.envsci.2010.09.010.
155. Kryza, M.; Dore, A.J.; Błaś, M.; Sobik, M. Modelling deposition and air concentration of reduced nitrogen in Poland and sensitivity to variability in annual meteorology. *Journal of Environmental Management* **2011**, *92*, 1225–1236. doi:10.1016/j.jenvman.2010.12.008.
156. Zhang, Y.; Dore, A.J.; Liu, X.; Zhang, F. Simulation of nitrogen deposition in the North China Plain by the FRAME model. *Biogeosciences* **2011**, *8*, 3319–3329. doi:10.5194/bg-8-3319-2011.
157. Meng, Z.; Seinfeld, J.H. Time scales to achieve atmospheric gas-aerosol equilibrium for volatile species. *Atmospheric Environment* **1996**, *30*, 2889–2900. doi:10.1016/1352-2310(95)00493-9.
158. Redington, A.L.; Derwent, R.G. Calculation of sulphate and nitrate aerosol concentrations over Europe using a Lagrangian dispersion model. *Atmospheric Environment* **2002**, *36*, 4425–4439. doi:10.1016/s1352-2310(02)00420-x.
159. van Pul, A.; Jaarsveld, H.V.; van der Meulen, T.; Velders, G. Ammonia concentrations in the Netherlands: spatially detailed measurements and model calculations. *Atmospheric Environment* **2004**, *38*, 4045–4055. Includes Special Issue Section on Results from the Austrian Project on Health Effects of Particulates (AUPHEP), doi:10.1016/j.atmosenv.2004.03.051.
160. van Jaarsveld, J. The Operational Priority Substances model. Technical report, Rijksinstituut voor Volksgezondheid en Milieu (RIVM), 2004.
161. van Pul, W.; van Jaarsveld, J.; Vellinga, O.; van den Broek, M.; Smits, M. The VELD experiment: An evaluation of the ammonia emissions and concentrations in an agricultural area. *Atmospheric Environment* **2008**, *42*, 8086–8095. doi:10.1016/j.atmosenv.2008.05.069.
162. Stolk, A.; Van Zanten, M.; Noordijk, H.; Van Jaarsveld, J.; van Pul, W. Measurements of Ammonia in Nature areas. Data of 2005-2007. techreport, Rijksinstituut voor Volksgezondheid en Milieu (RIVM), 2009.
163. Kruit, R.J.W.; Aben, J.; de Vries, W.; Sauter, F.; van der Swaluw, E.; van Zanten, M.C.; van Pul, W.A.J. Modelling trends in ammonia in the Netherlands over the period 1990–2014. *Atmospheric Environment* **2017**, *154*, 20–30. doi:10.1016/j.atmosenv.2017.01.031.
164. van der Swaluw, E.; Asman, W.A.; van Jaarsveld, H.; Hoogerbrugge, R. Wet deposition of ammonium, nitrate and sulfate in the Netherlands over the period 1992–2008. *Atmospheric Environment* **2011**, *45*, 3819–3826. doi:10.1016/j.atmosenv.2011.04.017.
165. Wen, D.; Lin, J.; Zhang, L.; Vet, R.; Moran, M. Modeling atmospheric ammonia and ammonium using a stochastic Lagrangian air quality model (STILT-Chem v0. 7). *Geoscientific Model Development* **2013**, *6*, 327–344. doi:10.5194/gmd-6-327-2013.
166. ApSimon, H.; Barker, B.; Kayin, S. Modelling studies of the atmospheric release and transport of ammonia in anticyclonic episodes. *Atmospheric Environment* **1994**, *28*, 665–678. doi:10.1016/1352-2310(94)90043-4.
167. Asman, W.A.; van Jaarsveld, H.A. A variable-resolution transport model applied for NHx in Europe. *Atmospheric Environment. Part A. General Topics* **1992**, *26*, 445–464. doi:10.1016/0960-1686(92)90329-j.
168. Asman, W. Modelling the atmospheric transport and deposition of ammonia and ammonium: an overview with special reference to Denmark. *Atmospheric Environment* **2001**, *35*, 1969–1983. doi:10.1016/s1352-2310(00)00548-3.
169. Dentener, F.J.; Crutzen, P.J. A three-dimensional model of the global ammonia cycle. *Journal of Atmospheric Chemistry* **1994**, *19*, 331–369. doi:10.1007/bf00694492.
170. Zimmermann, P.H. MOGUNTIA: A handy global tracer model. In *Air Pollution Modelling and its Applications VI*; van Dop, H., Ed.; Plenum, New York, 1988; pp. 593–608.
171. Simpson, D.; Benedictow, A.; Berge, H.; Bergström, R.; Emberson, L.D.; Fagerli, H.; Flechard, C.R.; Hayman, G.D.; Gauss, M.; Jonson, J.E.; Jenkin, M.E.; Nyíri, A.; Richter, C.; Semeena, V.S.; Tsyro, S.; Tuovinen, J.P.;

Valdebenito, A.; Wind, P. The EMEP MSC-W chemical transport model – technical description. *Atmospheric Chemistry and Physics* **2012**, *12*, 7825–7865. doi:10.5194/acp-12-7825-2012.

172. Barbu, A.; Segers, A.; Schaap, M.; Heemink, A.; Builtjes, P. A multi-component data assimilation experiment directed to sulphur dioxide and sulphate over Europe. *Atmospheric Environment* **2009**, *43*, 1622–1631. doi:10.1016/j.atmosenv.2008.12.005.
173. Byun, D.; Schere, K.L. Review of the Governing Equations, Computational Algorithms, and Other Components of the Models-3 Community Multiscale Air Quality (CMAQ) Modeling System. *Applied Mechanics Reviews* **2006**, *59*, 51. doi:10.1115/1.2128636.
174. Hoesly, R.M.; Smith, S.J.; Feng, L.; Klimont, Z.; Janssens-Maenhout, G.; Pitkanen, T.; Seibert, J.J.; Vu, L.; Andres, R.J.; Bolt, R.M.; Bond, T.C.; Dawidowski, L.; Kholod, N.; ichi Kurokawa, J.; Li, M.; Liu, L.; Lu, Z.; Moura, M.C.P.; O'Rourke, P.R.; Zhang, Q. Historical (1750–2014) anthropogenic emissions of reactive gases and aerosols from the Community Emissions Data System (CEDS). *Geoscientific Model Development* **2018**, *11*, 369–408. doi:10.5194/gmd-11-369-2018.
175. Crippa, M.; Solazzo, E.; Huang, G.; Guizzardi, D.; Koffi, E.; Muntean, M.; Schieberle, C.; Friedrich, R.; Janssens-Maenhout, G. High resolution temporal profiles in the Emissions Database for Global Atmospheric Research. *Scientific Data* **2020**, *7*. doi:10.1038/s41597-020-0462-2.
176. St-Pierre, R.P.; Cunje, A.; Au, A.; Baker, W.; Baratzadeh, P.; Barrigar, O.; Blain, D.; Czerwinski, A.; Dasné, S.; Earle, J.; Flemming, C.; Greenlaw, B.; Ha, C.; Kay, J.; Laurin, E.; LeBlanc-Power, G.; Lee, J.; Liang, C.; Lorente, M.; MacDonald, D.; Neitzert, F.; Osman, A.; Obeda, K.; Pratt, L.; Robert, C.; Smith, D.; Smyth, S.; Sullivan, B.; Taylor, B.; Thai, D.; Thiagarajan, A.; Tobin, S.; Tracey, K.; Zaki, H.; Zhao, N. *Canada's Air Pollutant Emissions Inventory Report 1990–2018*; Environment and Climate Change Canada: Gatineau, QC, Canada, 2020.
177. Reis, S.; Pinder, R.W.; Zhang, M.; Lijie, G.; Sutton, M.A. Reactive nitrogen in atmospheric emission inventories. *Atmospheric Chemistry and Physics* **2009**, *9*, 7657–7677. doi:10.5194/acp-9-7657-2009.
178. Velthof, G.; van Bruggen, C.; Groenestein, C.; de Haan, B.; Hoogeveen, M.; Huijsmans, J. A model for inventory of ammonia emissions from agriculture in the Netherlands. *Atmospheric Environment* **2012**, *46*, 248–255. doi:10.1016/j.atmosenv.2011.09.075.
179. Li, M.; Zhang, Q.; ichi Kurokawa, J.; Woo, J.H.; He, K.; Lu, Z.; Ohara, T.; Song, Y.; Streets, D.G.; Carmichael, G.R.; Cheng, Y.; Hong, C.; Huo, H.; Jiang, X.; Kang, S.; Liu, F.; Su, H.; Zheng, B. MIX: a mosaic Asian anthropogenic emission inventory under the international collaboration framework of the MICS-Asia and HTAP. *Atmospheric Chemistry and Physics* **2017**, *17*, 935–963. doi:10.5194/acp-17-935-2017.
180. Klimont, Z.; Cofala, J.; Schöpp, W.; Amann, M.; Streets, D.; Ichikawa, Y.; Fujita, S. Projections of SO2, NOx, NH3 and VOC Emissions in East Asia Up to 2030. *Water, Air, and Soil Pollution* **2001**, *130*, 193–198. doi:10.1023/a:1013886429786.
181. Ohara, T.; Akimoto, H.; Kurokawa, J.; Horii, N.; Yamaji, K.; Yan, X.; Hayasaka, T. An Asian emission inventory of anthropogenic emission sources for the period 1980–2020. *Atmospheric Chemistry and Physics* **2007**, *7*, 4419–4444. doi:10.5194/acp-7-4419-2007.
182. Yamaji, K.; Ohara, T.; Akimoto, H. Regional-specific emission inventory for NH3, N2O, and CH4 via animal farming in South, Southeast, and East Asia. *Atmospheric Environment* **2004**, *38*, 7111–7121. doi:10.1016/j.atmosenv.2004.06.045.
183. Dianwu, Z.; Anpu, W. Estimation of anthropogenic ammonia emissions in asia. *Atmospheric Environment* **1994**, *28*, 689–694. doi:10.1016/1352-2310(94)90045-0.
184. Kurokawa, J.; Ohara, T. Long-term historical trends in air pollutant emissions in Asia: Regional Emission inventory in ASia (REAS) version 3.1. *Atmospheric Chemistry and Physics Discussions* **2019**, *2019*, 1–51. doi:10.5194/acp-2019-1122.
185. Kurokawa, J.; Ohara, T.; Morikawa, T.; Hanayama, S.; Janssens-Maenhout, G.; Fukui, T.; Kawashima, K.; Akimoto, H. Emissions of air pollutants and greenhouse gases over Asian regions during 2000–2008: Regional Emission inventory in ASia (REAS) version 2. *Atmospheric Chemistry and Physics* **2013**, *13*, 11019–11058. doi:10.5194/acp-13-11019-2013.
186. Marais, E.A.; Wiedinmyer, C. Air Quality Impact of Diffuse and Inefficient Combustion Emissions in Africa (DICE-Africa). *Environmental Science & Technology* **2016**, *50*, 10739–10745. doi:10.1021/acs.est.6b02602.
187. Battye, W.; Aneja, V.P.; Roelle, P.A. Evaluation and improvement of ammonia emissions inventories. *Atmospheric Environment* **2003**, *37*, 3873–3883. doi:10.1016/S1352-2310(03)00343-1.

188. Zheng, J.Y.; Yin, S.S.; Kang, D.W.; Che, W.W.; Zhong, L.J. Development and uncertainty analysis of a high-resolution NH_3 emissions inventory and its implications with precipitation over the Pearl River Delta region, China. *Atmospheric Chemistry and Physics* **2012**, *12*, 7041–7058. doi:10.5194/acp-12-7041-2012.
189. Yu, X.; Shen, L.; Hou, X.; Yuan, L.; Pan, Y.; An, J.; Yan, S. High-resolution anthropogenic ammonia emission inventory for the Yangtze River Delta, China. *Chemosphere* **2020**, *251*, 126342. doi:10.1016/j.chemosphere.2020.126342.
190. Asman, W.A.H.; Sutton, M.A.; Schjorring, J.K. Ammonia: emission, atmospheric transport and deposition. *New Phytologist* **1998**, *139*, 27–48. doi:10.1046/j.1469-8137.1998.00180.x.
191. Battye, R.; Battye, W.; Overcash, C.; Fudge, S. Development and selection of ammonia emission factors. Technical report, US Environmental Protection Agency, Atmospheric Research and Exposure Assessment Laboratory, 1994.
192. Aneja, V.P.; Murray, G.C.; Southerland, J. Atmospheric nitrogen compounds: emissions, transport, transformation, deposition and assessment. *EM* **1998**, *1998*, 22–25.
193. Aneja, V.P.; Chauhan, J.P.; Walker, J.T. Characterization of atmospheric ammonia emissions from swine waste storage and treatment lagoons. *Journal of Geophysical Research: Atmospheres* **2000**, *105*, 11535–11545. doi:10.1029/2000JD900066.
194. Aneja, V.P.; Roelle, P.A.; Murray, G.C.; Southerland, J.; Erisman, J.W.; Fowler, D.; Asman, W.A.; Patni, N. Atmospheric nitrogen compounds II: emissions, transport, transformation, deposition and assessment. *Atmospheric Environment* **2001**, *35*, 1903–1911. doi:10.1016/s1352-2310(00)00543-4.
195. Aneja, V.P.; Nelson, D.R.; Roelle, P.A.; Walker, J.T.; Battye, W. Agricultural ammonia emissions and ammonium concentrations associated with aerosols and precipitation in the southeast United States. *Journal of Geophysical Research: Atmospheres* **2003**, *108*, 12.1–12.11. doi:10.1029/2002JD002271.
196. Sutton, M.A.; Reis, S.; Riddick, S.N.; Dragosits, U.; Nemitz, E.; Theobald, M.R.; Tang, Y.S.; Braban, C.F.; Vieno, M.; Dore, A.J.; Mitchell, R.F.; Wanless, S.; Daunt, F.; Fowler, D.; Blackall, T.D.; Milford, C.; Flechard, C.R.; Loubet, B.; Massad, R.; Cellier, P.; Personne, E.; Coheur, P.F.; Clarisse, L.; Damme, M.V.; Ngadi, Y.; Clerbaux, C.; Skjøth, C.A.; Geels, C.; Hertel, O.; Kruit, R.J.W.; Pinder, R.W.; Bash, J.O.; Walker, J.T.; Simpson, D.; Horváth, L.; Misselbrook, T.H.; Bleeker, A.; Dentener, F.; de Vries, W. Towards a climate-dependent paradigm of ammonia emission and deposition. *Philosophical Transactions of the Royal Society B: Biological Sciences* **2013**, *368*, 20130166. doi:10.1098/rstb.2013.0166.
197. Olivier, J.; Bouwman, A.; der Hoek, K.V.; Berdowski, J. Global air emission inventories for anthropogenic sources of NOx, NH3 and N2O in 1990. *Environmental Pollution* **1998**, *102*, 135–148. doi:10.1016/s0269-7491(98)80026-2.
198. van Der Hoek, K. Estimating ammonia emission factors in Europe: Summary of the work of the UNECE ammonia expert panel. *Atmospheric Environment* **1998**, *32*, 315–316. doi:10.1016/S1352-2310(97)00168-4.
199. Li, C.; Martin, R.V.; Shephard, M.W.; Cady-Pereira, K.; Cooper, M.J.; Kaiser, J.; Lee, C.J.; Zhang, L.; Henze, D.K. Assessing the Iterative Finite Difference Mass Balance and 4D-Var Methods to Derive Ammonia Emissions Over North America Using Synthetic Observations. *Journal of Geophysical Research: Atmospheres* **2019**, *124*, 4222–4236. doi:10.1029/2018jd030183.
200. Zhang, L.; Chen, Y.; Zhao, Y.; Henze, D.K.; Zhu, L.; Song, Y.; Paulot, F.; Liu, X.; Pan, Y.; Lin, Y.; Huang, B. Agricultural ammonia emissions in China: reconciling bottom-up and top-down estimates. *Atmospheric Chemistry and Physics* **2018**, *18*, 339–355. doi:10.5194/acp-18-339-2018.
201. Bassett, M.; Seinfeld, J.H. Atmospheric equilibrium model of sulfate and nitrate aerosols. *Atmospheric Environment (1967)* **1983**, *17*, 2237–2252. doi:10.1016/0004-6981(83)90221-4.
202. Bassett, M.E.; Seinfeld, J.H. Atmospheric equilibrium model of sulfate and nitrate aerosols—II. Particle size analysis. *Atmospheric Environment (1967)* **1984**, *18*, 1163–1170. doi:10.1016/0004-6981(84)90147-1.
203. Binkowski, F.S.; Shankar, U. The Regional Particulate Matter Model: 1. Model description and preliminary results. *Journal of Geophysical Research* **1995**, *100*, 26191. doi:10.1029/95jd02093.
204. Binkowski, F.S.; Roselle, S.J. Models-3 Community Multiscale Air Quality (CMAQ) model aerosol component 1. Model description. *Journal of Geophysical Research: Atmospheres* **2003**, *108*. doi:10.1029/2001jd001409.
205. Pilinis, C.; Seinfeld, J.H. Continued development of a general equilibrium model for inorganic multicomponent atmospheric aerosols. *Atmospheric Environment (1967)* **1987**, *21*, 2453–2466. doi:10.1016/0004-6981(87)90380-5.

206. Kim, Y.P.; Seinfeld, J.H.; Saxena, P. Atmospheric Gas-Aerosol Equilibrium I. Thermodynamic Model. *Aerosol Science and Technology* **1993**, *19*, 157–181. doi:10.1080/02786829308959628.
207. Wexler, A.S.; Seinfeld, J.H. Second-generation inorganic aerosol model. *Atmospheric Environment. Part A. General Topics* **1991**, *25*, 2731–2748. doi:10.1016/0960-1686(91)90203-j.
208. Clegg, S.L.; Brimblecombe, P.; Wexler, A.S. Thermodynamic Model of the System H+ – NH4+ – SO42- – NO3- – H2O at Tropospheric Temperatures. *The Journal of Physical Chemistry A* **1998**, *102*, 2137–2154. doi:10.1021/jp973042r.
209. Ansari, A. Prediction of multicomponent inorganic atmospheric aerosol behavior. *Atmospheric Environment* **1999**, *33*, 745–757. doi:10.1016/s1352-2310(98)00221-0.
210. Nenes, A.; Pandis, S.N.; Pilinis, C. ISORROPIA: A new thermodynamic equilibrium model for multiphase multicomponent inorganic aerosols. *Aquatic geochemistry* **1998**, *4*, 123–152. doi:10.1023/A:1009604003981.
211. Fountoukis, C.; Nenes, A. ISORROPIA II: a computationally efficient thermodynamic equilibrium model for K+–Ca2+–Mg2+–NH4+–Na+–SO42- –NO3- –Cl- –H2O aerosols. *Atmospheric Chemistry and Physics* **2007**, *7*, 4639–4659. doi:10.5194/acp-7-4639-2007.
212. Jacobson, M.Z.; Tabazadeh, A.; Turco, R.P. Simulating equilibrium within aerosols and nonequilibrium between gases and aerosols. *Journal of Geophysical Research: Atmospheres* **1996**, *101*, 9079–9091. doi:10.1029/96jd00348.
213. Jacobson, M.Z. Studying the effects of calcium and magnesium on size-distributed nitrate and ammonium with EQUISOLV II. *Atmospheric Environment* **1999**, *33*, 3635–3649. doi:10.1016/s1352-2310(99)00105-3.
214. Zaveri, R.A.; Easter, R.C.; Peters, L.K. A computationally efficient Multicomponent Equilibrium Solver for Aerosols (MESA). *Journal of Geophysical Research* **2005**, *110*. doi:10.1029/2004jd005618.
215. Topping, D.O.; McFiggans, G.B.; Coe, H. A curved multi-component aerosol hygroscopicity model framework: Part 1 – Inorganic compounds. *Atmospheric Chemistry and Physics* **2005**, *5*, 1205–1222. doi:10.5194/acp-5-1205-2005.
216. Amundson, N.R.; Caboussat, A.; He, J.W.; Martynenko, A.V.; Savarin, V.B.; Seinfeld, J.H.; Yoo, K.Y. A new inorganic atmospheric aerosol phase equilibrium model (UHAERO). *Atmospheric Chemistry and Physics* **2006**, *6*, 975–992. doi:10.5194/acp-6-975-2006.
217. Pilinis, C. Modeling atmospheric aerosols using thermodynamic arguments - A Review. *Global Nest: The International Journal* **1999**, *1*, 5–13. doi:10.30955/gnj.000103.
218. Zhang, Y.; Seigneur, C.; Seinfeld, J.H.; Jacobson, M.; Clegg, S.L.; Binkowski, F.S. A comparative review of inorganic aerosol thermodynamic equilibrium modules: similarities, differences, and their likely causes. *Atmospheric Environment* **2000**, *34*, 117–137. doi:10.1016/s1352-2310(99)00236-8.
219. Jacobson, M.Z. Numerical Techniques to Solve Condensational and Dissolutional Growth Equations When Growth is Coupled to Reversible Reactions. *Aerosol Science and Technology* **1997**, *27*, 491–498. doi:10.1080/02786829708965489.
220. Jacobson, M.Z. Development and application of a new air pollution modeling system—II. Aerosol module structure and design. *Atmospheric Environment* **1997**, *31*, 131–144. doi:10.1016/1352-2310(96)00202-6.
221. Meng, Z.; Dabdub, D.; Seinfeld, J.H. Size-resolved and chemically resolved model of atmospheric aerosol dynamics. *Journal of Geophysical Research: Atmospheres* **1998**, *103*, 3419–3435. doi:10.1029/97jd02796.
222. Sun, Q.; Wexler, A.S. Modeling urban and regional aerosols—condensation and evaporation near acid neutrality. *Atmospheric Environment* **1998**, *32*, 3527–3531. doi:10.1016/s1352-2310(98)00059-4.
223. Pilinis, C.; Capaldo, K.P.; Nenes, A.; Pandis, S.N. MADM-A New Multicomponent Aerosol Dynamics Model. *Aerosol Science and Technology* **2000**, *32*, 482–502. doi:10.1080/027868200303597.
224. Capaldo, K.P.; Pilinis, C.; Pandis, S.N. A computationally efficient hybrid approach for dynamic gas/aerosol transfer in air quality models. *Atmospheric Environment* **2000**, *34*, 3617–3627. doi:10.1016/s1352-2310(00)00092-3.
225. Koo, B.; Gaydos, T.M.; Pandis, S.N. Evaluation of the Equilibrium, Dynamic, and Hybrid Aerosol Modeling Approaches. *Aerosol Science and Technology* **2003**, *37*, 53–64. doi:10.1080/02786820300893.
226. Gaydos, T.M.; Koo, B.; Pandis, S.N.; Chock, D.P. Development and application of an efficient moving sectional approach for the solution of the atmospheric aerosol condensation/evaporation equations. *Atmospheric Environment* **2003**, *37*, 3303–3316. doi:10.1016/s1352-2310(03)00267-x.

227. Tombette, M.; Sportisse, B. Aerosol modeling at a regional scale: Model-to-data comparison and sensitivity analysis over Greater Paris. *Atmospheric Environment* **2007**, *41*, 6941–6950. doi:10.1016/j.atmosenv.2006.10.037.
228. Paulot, F.; Jacob, D.J.; Henze, D.K. Sources and Processes Contributing to Nitrogen Deposition: An Adjoint Model Analysis Applied to Biodiversity Hotspots Worldwide. *Environmental Science & Technology* **2013**, *47*, 3226–3233. doi:10.1021/es3027727.
229. Behera, S.N.; Sharma, M.; Aneja, V.P.; Balasubramanian, R. Ammonia in the atmosphere: a review on emission sources, atmospheric chemistry and deposition on terrestrial bodies. *Environmental Science and Pollution Research* **2013**, *20*, 8092–8131. doi:10.1007/s11356-013-2051-9.
230. Massad, R.S.; Nemitz, E.; Sutton, M.A. Review and parameterisation of bi-directional ammonia exchange between vegetation and the atmosphere. *Atmospheric Chemistry and Physics* **2010**, *10*, 10359–10386. doi:10.5194/acp-10-10359-2010.
231. Zhang, L.; Wright, L.P.; Asman, W.A.H. Bi-directional air-surface exchange of atmospheric ammonia: A review of measurements and a development of a big-leaf model for applications in regional-scale air-quality models. *Journal of Geophysical Research* **2010**, *115*. doi:10.1029/2009jd013589.
232. Langford, A.O.; Fehsenfeld, F.C. Natural Vegetation as a Source or Sink for Atmospheric Ammonia: A Case Study. *Science* **1992**, *255*, 581–583. doi:10.1126/science.255.5044.581.
233. Sutton, M.A.; Nemitz, E.; Milford, C.; Campbell, C.; Erisman, J.W.; Hensen, A.; Cellier, P.; David, M.; Loubet, B.; Personne, E.; Schjoerring, J.K.; Mattsson, M.; Dorsey, J.R.; Gallagher, M.W.; Horvath, L.; Weidinger, T.; Meszaros, R.; Dämmgen, U.; Neftel, A.; Herrmann, B.; Lehman, B.E.; Flechard, C.; Burkhardt, J. Dynamics of ammonia exchange with cut grassland: synthesis of results and conclusions of the GRAMINAE Integrated Experiment. *Biogeosciences* **2009**, *6*, 2907–2934. doi:10.5194/bg-6-2907-2009.
234. Sutton, M.; Nemitz, E.; Erisman, J.; Beier, C.; Bahl, K.B.; Cellier, P.; de Vries, W.; Cotrufo, F.; Skiba, U.; Marco, C.D.; Jones, S.; Laville, P.; Soussana, J.; Loubet, B.; Twigg, M.; Famulari, D.; Whitehead, J.; Gallagher, M.; Neftel, A.; Flechard, C.; Herrmann, B.; Calanca, P.; Schjoerring, J.; Daemmgen, U.; Horvath, L.; Tang, Y.; Emmett, B.; Tietema, A.; Peñuelas, J.; Kesik, M.; Brueggemann, N.; Pilegaard, K.; Vesala, T.; Campbell, C.; Olesen, J.; Dragosits, U.; Theobald, M.; Levy, P.; Mobbs, D.; Milne, R.; Viovy, N.; Vuichard, N.; Smith, J.; Smith, P.; Bergamaschi, P.; Fowler, D.; Reis, S. Challenges in quantifying biosphere–atmosphere exchange of nitrogen species. *Environmental Pollution* **2007**, *150*, 125–139. doi:10.1016/j.envpol.2007.04.014.
235. Sutton, M.A.; Burkhardt, J.K.; Guerin, D.; Nemitz, E.; Fowler, D. Development of resistance models to describe measurements of bi-directional ammonia surface–atmosphere exchange. *Atmospheric Environment* **1998**, *32*, 473–480. doi:10.1016/s1352-2310(97)00164-7.
236. Nemitz, E.; Milford, C.; Sutton, M.A. A two-layer canopy compensation point model for describing bi-directional biosphere-atmosphere exchange of ammonia. *Quarterly Journal of the Royal Meteorological Society* **2001**, *127*, 815–833. doi:10.1002/qj.49712757306.
237. Cooter, E.J.; Bash, J.O.; Walker, J.T.; Jones, M.; Robarge, W. Estimation of NH3 bi-directional flux from managed agricultural soils. *Atmospheric Environment* **2010**, *44*, 2107–2115. doi:10.1016/j.atmosenv.2010.02.044.
238. Kruit, R.J.W.; Schaap, M.; Sauter, F.J.; van Zanten, M.C.; van Pul, W.A.J. Modeling the distribution of ammonia across Europe including bi-directional surface–atmosphere exchange. *Biogeosciences* **2012**, *9*, 5261–5277. doi:10.5194/bg-9-5261-2012.
239. Bash, J.O.; Cooter, E.J.; Dennis, R.L.; Walker, J.T.; Pleim, J.E. Evaluation of a regional air-quality model with bidirectional NH3 exchange coupled to an agroecosystem model. *Biogeosciences* **2013**, *10*, 1635–1645. doi:10.5194/bg-10-1635-2013.
240. Pleim, J.E.; Bash, J.O.; Walker, J.T.; Cooter, E.J. Development and evaluation of an ammonia bidirectional flux parameterization for air quality models. *Journal of Geophysical Research: Atmospheres* **2013**, *118*, 3794–3806. doi:10.1002/jgrd.50262.
241. Park, R.J. Natural and transboundary pollution influences on sulfate-nitrate-ammonium aerosols in the United States: Implications for policy. *Journal of Geophysical Research* **2004**, *109*. doi:10.1029/2003jd004473.
242. Luo, G.; Yu, F.; Schwab, J. Revised treatment of wet scavenging processes dramatically improves GEOS-Chem 12.0.0 simulations of surface nitric acid, nitrate, and ammonium over the United States. *Geoscientific Model Development* **2019**, *12*, 3439–3447. doi:10.5194/gmd-12-3439-2019.

243. Luo, G.; Yu, F.; Moch, J.M. Further improvement of wet process treatments in GEOS-Chem v12.6.0: impact on global distributions of aerosols and aerosol precursors. *Geoscientific Model Development* **2020**, *13*, 2879–2903. doi:10.5194/gmd-13-2879-2020.
244. van Damme M..; W., E.J.; L., C.; E., D.; S., W.; C., C.; J., D.A.; P.-F., C. Worldwide spatiotemporal atmospheric ammonia (NH3) columns variability revealed by satellite. *Geophysical Research Letters* **2015**, *42*, 8660–8668. doi:10.1002/2015GL065496.
245. Xing, J.; Pleim, J.; Mathur, R.; Pouliot, G.; Hogrefe, C.; Gan, C.M.; Wei, C. Historical gaseous and primary aerosol emissions in the United States from 1990 to 2010. *Atmospheric Chemistry and Physics* **2013**, *13*, 7531–7549. doi:10.5194/acp-13-7531-2013.
246. Li, Y.; Thompson, T.M.; Damme, M.V.; Chen, X.; Benedict, K.B.; Shao, Y.; Day, D.; Boris, A.; Sullivan, A.P.; Ham, J.; Whitburn, S.; Clarisse, L.; Coheur, P.F.; Jr., J.L.C. Temporal and spatial variability of ammonia in urban and agricultural regions of northern Colorado, United States. *Atmospheric Chemistry and Physics* **2017**, *17*, 6197–6213. doi:10.5194/acp-17-6197-2017.
247. Yan, X.; Akimoto, H.; Ohara, T. Estimation of nitrous oxide, nitric oxide and ammonia emissions from croplands in East, Southeast and South Asia. *Global Change Biology* **2003**, *9*, 1080–1096. doi:10.1046/j.1365-2486.2003.00649.x.
248. Wang, X.; Mauzerall, D.L.; Hu, Y.; Russell, A.G.; Larson, E.D.; Woo, J.H.; Streets, D.G.; Guenther, A. A high-resolution emission inventory for eastern China in 2000 and three scenarios for 2020. *Atmospheric Environment* **2005**, *39*, 5917–5933. doi:10.1016/j.atmosenv.2005.06.051.
249. Liu, L.; Zhang, X.; Xu, W.; Liu, X.; Li, Y.; Lu, X.; Zhang, Y.; Zhang, W. Temporal characteristics of atmospheric ammonia and nitrogen dioxide over China based on emission data, satellite observations and atmospheric transport modeling since 1980. *Atmospheric Chemistry and Physics* **2017**, *17*, 9365–9378. doi:10.5194/acp-17-9365-2017.
250. Pan, Y.; Tian, S.; Zhao, Y.; Zhang, L.; Zhu, X.; Gao, J.; Huang, W.; Zhou, Y.; Song, Y.; Zhang, Q.; Wang, Y. Identifying Ammonia Hotspots in China Using a National Observation Network. *Environmental Science & Technology* **2018**, *52*, 3926–3934. doi:10.1021/acs.est.7b05235.
251. Langford, A.; Fehsenfeld, F.; Zachariassen, J.; Schimel, D. Gaseous ammonia fluxes and background concentrations in terrestrial ecosystems of the United States. *Global Biogeochemical Cycles* **1992**, *6*, 459–483. doi:10.1029/92GB02123.
252. Alkezweeny, A.; Laws, G.; Jones, W. Aircraft and ground measurements of ammonia in Kentucky. *Atmospheric Environment (1967)* **1986**, *20*, 357–360. doi:10.1016/0004-6981(86)90038-7.
253. Erisman, J.W.; Vermetten, A.W.; Asman, W.A.; Waijers-Ijpelaan, A.; Slanina, J. Vertical distribution of gases and aerosols: The behaviour of ammonia and related components in the lower atmosphere. *Atmospheric Environment (1967)* **1988**, *22*, 1153–1160. doi:10.1016/0004-6981(88)90345-9.
254. Buijsman, E.; Aben, J.M.; Elzakker, B.G.V.; Mennen, M.G. An automatic atmospheric ammonia network in the Netherlands set-up and results. *Atmospheric Environment* **1998**, *32*, 317–324. doi:10.1016/s1352-2310(97)00233-1.
255. Walker, J.; Whitall, D.R.; Robarge, W.; Paerl, H.W. Ambient ammonia and ammonium aerosol across a region of variable ammonia emission density. *Atmospheric Environment* **2004**, *38*, 1235–1246. doi:10.1016/j.atmosenv.2003.11.027.
256. Parmar, R.; Satsangi, G.; Lakhani, A.; Srivastava, S.; Prakash, S. Simultaneous measurements of ammonia and nitric acid in ambient air at Agra (27°10′N and 78°05′E) (India). *Atmospheric Environment* **2001**, *35*, 5979–5988. doi:10.1016/s1352-2310(00)00394-0.
257. Pierson, W.R.; Brachaczek, W.W.; Gorse, R.A.; Japar, S.M.; Norbeck, J.M. On the acidity of dew. *Journal of Geophysical Research: Atmospheres* **1986**, *91*, 4083–4096. doi:10.1029/JD091iD03p04083.
258. Perrino, C.; Catrambone, M.; Bucchianico, A.D.M.D.; Allegrini, I. Gaseous ammonia in the urban area of Rome, Italy and its relationship with traffic emissions. *Atmospheric Environment* **2002**, *36*, 5385–5394. doi:10.1016/s1352-2310(02)00469-7.
259. Ianniello, A.; Spataro, F.; Esposito, G.; Allegrini, I.; Rantica, E.; Ancora, M.P.; Hu, M.; Zhu, T. Occurrence of gas phase ammonia in the area of Beijing (China). *Atmospheric Chemistry and Physics* **2010**, *10*, 9487–9503. doi:10.5194/acp-10-9487-2010.

260. Gong, L.; Lewicki, R.; Griffin, R.J.; Flynn, J.H.; Lefer, B.L.; Tittel, F.K. Atmospheric ammonia measurements in Houston, TX using an external-cavity quantum cascade laser-based sensor. *Atmospheric Chemistry and Physics* **2011**, *11*, 9721–9733. doi:10.5194/acp-11-9721-2011.
261. Pandolfi, M.; Amato, F.; Reche, C.; Alastuey, A.; Otjes, R.P.; Blom, M.J.; Querol, X. Summer ammonia measurements in a densely populated Mediterranean city. *Atmospheric Chemistry and Physics* **2012**, *12*, 7557–7575. doi:10.5194/acp-12-7557-2012.
262. Sharma, S.K.; Mandal, T.K.; Rohtash.; Kumar, M.; Gupta, N.C.; Pathak, H.; Harit, R.C.; Saxena, M. Measurement of Ambient Ammonia over the National Capital Region of Delhi, India. *MAPAN* **2014**, *29*, 165–173. doi:10.1007/s12647-014-0098-9.
263. Wang, S.; Nan, J.; Shi, C.; Fu, Q.; Gao, S.; Wang, D.; Cui, H.; Saiz-Lopez, A.; Zhou, B. Atmospheric ammonia and its impacts on regional air quality over the megacity of Shanghai, China. *Scientific Reports* **2015**, *5*. doi:10.1038/srep15842.
264. Ni, J. Mechanistic models of ammonia release from liquid manure: a review. *Journal of Agricultural Engineering Research* **1999**, *72*, 1–17. doi:10.1006/jaer.1998.0342.
265. Sommer, S.G.; Olesen, J.E.; Christensen, B.T. Effects of temperature, wind speed and air humidity on ammonia volatilization from surface applied cattle slurry. *The Journal of Agricultural Science* **1991**, *117*, 91–100. doi:10.1017/S0021859600079016.
266. Robarge, W.P.; Walker, J.T.; McCulloch, R.B.; Murray, G. Atmospheric concentrations of ammonia and ammonium at an agricultural site in the southeast United States. *Atmospheric Environment* **2002**, *36*, 1661–1674. doi:10.1016/s1352-2310(02)00171-1.
267. Bari, A.; Ferraro, V.; Wilson, L.R.; Luttinger, D.; Husain, L. Measurements of gaseous HONO, HNO3, SO2, HCl, NH3, particulate sulfate and PM2.5 in New York, NY. *Atmospheric Environment* **2003**, *37*, 2825–2835. doi:10.1016/s1352-2310(03)00199-7.
268. Anatolaki, C.; Tsitouridou, R. Atmospheric deposition of nitrogen, sulfur and chloride in Thessaloniki, Greece. *Atmospheric Research* **2007**, *85*, 413–428. doi:10.1016/j.atmosres.2007.02.010.
269. Wyers, G.; Duyzer, J. Micrometeorological measurement of the dry deposition flux of sulphate and nitrate aerosols to coniferous forest. *Atmospheric Environment* **1997**, *31*, 333–343. doi:10.1016/S1352-2310(96)00188-4.
270. Hoell, J.M.; Harward, C.N.; Williams, B.S. Remote infrared heterodyne radiometer measurements of atmospheric ammonia profiles. *Geophysical Research Letters* **1980**, *7*, 313–316. doi:10.1029/gl007i005p00313.
271. Cadle, S.; Countess, R.; Kelly, N. Nitric acid and ammonia in urban and rural locations. *Atmospheric Environment (1967)* **1982**, *16*, 2501–2506. doi:10.1016/0004-6981(82)90141-x.
272. Burkhardt, J.; Sutton, M.; Milford, C.; Storeton-West, R.; Fowler, D. Ammonia concentrations at a site in Southern Scotland from 2yr of continuous measurements. *Atmospheric Environment* **1998**, *32*, 325–331. doi:10.1016/s1352-2310(97)00198-2.
273. Yao, X.; Zhang, L. Trends in atmospheric ammonia at urban, rural, and remote sites across North America. *Atmospheric Chemistry and Physics* **2016**, *16*, 11465–11475. doi:10.5194/acp-16-11465-2016.
274. Hu, Q.; Zhang, L.; Evans, G.J.; Yao, X. Variability of atmospheric ammonia related to potential emission sources in downtown Toronto, Canada. *Atmospheric Environment* **2014**, *99*, 365–373. doi:10.1016/j.atmosenv.2014.10.006.
275. Alebic-Juretic, A. Airborne ammonia and ammonium within the Northern Adriatic area, Croatia. *Environmental Pollution* **2008**, *154*, 439–447. doi:10.1016/j.envpol.2007.11.029.
276. Tang, Y.S.; Dragosits, U.; van Dijk, N.; Love, L.; Simmons, I.; Sutton, M.A. Assessment of Ammonia and Ammonium Trends and Relationship to Critical Levels in the UK National Ammonia Monitoring Network (NAMN). In *Atmospheric Ammonia*; Springer Netherlands, 2009; pp. 187–194. doi:10.1007/978-1-4020-9121-6_13.
277. Ferm, M.; Hellsten, S. Trends in atmospheric ammonia and particulate ammonium concentrations in Sweden and its causes. *Atmospheric Environment* **2012**, *61*, 30–39. doi:10.1016/j.atmosenv.2012.07.010.
278. Sutton, M.A.; Asman, W.A.H.; Ellermann, T.; Jaarsveld, J.A.V.; Acker, K.; Aneja, V.; Duyzer, J.; Horvath, L.; Paramonov, S.; Mitosinkova, M.; Tang, Y.S.; Achermann, B.; Gauger, T.; Bartniki, J.; Neftel, A.; Erisman, J.W. Establishing the Link between Ammonia Emission Control and Measurements of Reduced Nitrogen Concentrations and Deposition. *Environmental Monitoring and Assessment* **2003**, *82*, 149–185. doi:10.1023/a:1021834132138.